

ISSN:2538-516X

Journal of
**Civil
Engineering
Researchers**

Volume: 4; Number: 4; December 2022

Chief Editorial:
Morteza Jamshidi

Managing Editor:
Kamyar Bagherineghad



J-Researchers



Volume 4, Number 4, December 2022

Contents

1. **Experimental Study of Mechanical Properties of Geopolymer Concrete as Green Concrete with a Sustainable Development Approach in the Construction Industry, Under High Temperature** 1-11
Mohammadhossein Mansourghanaei, Morteza Biklaryan, Alireza Mardookhpour
2. **Comparative study of numerical methods used in prediction of post-crack behavior of waffle slabs** 12-19
Alireza Sheikhnasiri
3. **I Investigating the compressive and tensile strength of concrete containing recycled aggregate with polypropylene fibres** 20-32
Donya Khazraie, Hossein Razzaghi
4. **The role of advanced crisis management in providing relief during an earthquake using the location of vulnerable areas based on the risk matrix (case study: Lahijan city)** 33-40
Sahebeh Kheirkhah Ghorbani
5. **Analytical and Experimental Study of Load-bearing columns Made of Lightweight Concrete** 41-50
Ghasem Azizi, Mohsen Abzan
6. **Parametric study of two-layer corrugated steel shear wall under lateral load** 51-59
Saeid Ostai



Experimental Study of Mechanical Properties of Geopolymer Concrete as Green Concrete with a Sustainable Development Approach in the Construction Industry, Under High Temperature

Mohammadhossein Mansourghanaei^{a*}, Morteza Biklaryan^a, A. Mardookhpour^b

^aDepartment of Civil Engineering, Chalous Branch, Islamic Azad University, Chalous, Iran

^bDepartment of Civil Engineering, Lahijan Branch, Islamic Azad University, Lahijan, Iran

Journals-Researchers use only: Received date: 2022.10.20; revised date: 2022.11.15; accepted date: 2022.11.20

Abstract

Today, the use of processed mineral materials in concrete to improve mechanical properties and durability has opened a wide field of vision for researchers in the structural sciences. On the other hand, preserving the environment by reducing the toxic gas of carbon dioxide caused by cement production is one of the concerns of scientists. In this regard, minerals containing abundant aluminosilicate particles and active alkali solution (AAS) replaced ordinary cement in concrete and led to the production of geopolymer concrete (GPC). The composition and reactivity of these materials produce a strong adhesive material that in combination with other concrete components, causes the final strength of GPC. High temperatures weaken the concrete against loads by damaging the structure of hydrated gels in concrete. GPC has better fire resistance than OPCC due to its density in its microstructure. In the current study, Granulated Blast Furnace Slag (GBFS)-based GPC was used with 0-2% polyolefin fibers (POFs) and 0-8% Nano silica (NS) to improve its structure. After curing the specimens under dry conditions at a temperature of 60 °C in an oven, they were subjected to Compressive strength, Modulus of elasticity and Weight Loss tests to evaluate their mechanical properties. All tests were performed at 90 days of age under ambient temperature (20 °C) and high temperature (500 °C). The addition of NS enhanced the whole properties of the GBFS-based GPC. Addition of up to 8% NS to the GPC composition at 20% temperature improved the modulus of elasticity test results by 13.42% and the compressive strength up to 21.94% by 11.58%. Addition of up to 2% of POFs to the GPC composition resulted in an improvement, modulus of elasticity of 07.05% and a decrease in compressive strength of up to 22.49%. Apply the lowest (0.061%) and highest (0.12%) weight loss percentage of concrete samples under 500% heat, belonging to scheme 4 (including GPC containing 8% NS) and scheme 6 (including GPC containing 2% POFs) Came. In the following, by conducting the Slag, Scanning Electron Microscope (SEM) analysis, a microstructure investigation was carried out on the concrete samples. In addition to their overlapping with each other, the results indicate the GPC superiority over the regular concrete. Besides, it demonstrated the positive influence of NS addition on the concert microstructure. © 2017 Journals-Researchers. All rights reserved. (DOI: <https://doi.org/10.52547/JCER.4.4.1>)

Keywords : Geopolymer Concrete, Polyolefin Fibers, Nano Silica, Granulated Blast Furnace Slag, Scanning Electron Microscope.

* Corresponding author. Tel: +989121712070; E-mail: Mhm.Ghanaei@iauc.ac.ir

1. Introduction

Currently, considering global trends and challenges, as well as the UN¹ sustainable development goals and the ESG² plan, the development of geopolymer binders for the production of GPC has become an urgent area of construction science [1]. GPC is one of the innovative eco-friendly materials that has gained the attention of many researchers in the sustainable development of the construction industry [2]. GPC is a new material in the construction industry, with different chemical compositions and reactions involved in a binding material. The pozzolanic materials (industrial waste like fly ash, ground granulated blast furnace slag), which contain high silica and alumina, work as binding materials in the mix. GPC is economical, low energy consumption, thermally stable, easily workable, eco-friendly, cementless, and durable [3]. GPC is an environmental friendly concrete as it relies on minor treated natural materials or industrial wastes like (Fly ash, GBFS and silica fumes etc) which are having high alumina and silica content, to significantly reduce the carbon footprints [4]. GPC is produced from the geopolymerization process, in which molecules known as oligomers integrate to form geopolymer networks with covalent bonding [5]. Materials research has shown GPC has the potential to significantly improve the sustainability of concrete construction [6]. GPC has superior mechanical and durability properties compared to ordinary Portland cement (OPCC) concrete [7]. Geopolymers are novel cementitious materials that have the potential to replace conventional Portland cement composites completely, the production of geopolymer composites has a lower carbon footprint and uses less energy than the production of Portland cement [8]. Production and utilization of cement severely affect the environment due to the emission of various gases, the application of GPC plays a vital role in reducing this flaw [9]. To reduce CO₂ emissions by 55% by 2030, applying sustainable and energy-efficient materials like GPC containing Phase change materials for infrastructure development is necessary [10]. GPCs have lower CO₂ emissions than conventional concrete and Portland cement [10-13,2]. GPC is a perfect alternative to conventional cement

concrete [14]. In the process of substituting OPCC concrete production, the development of GPC is considered as the major breakthrough [15]. GPC is a high-performance concrete [16]. Geopolymer or alkali-activated binders are emerging as a potential green sustainable alternative for OPCC [17]. Geopolymer composite is a new cementitious material, and it appears to be a potential replacement for conventional cement concrete [18]. Geopolymers are cementitious materials known for their environmental benefits and comparable characteristics to conventional Portland cement [19]. Compressive strength is an important property of all concrete composites, including GPC [20]. SEM analysis exhibited that the geopolymer matrix contained more dispersed small-sized pores which indicate a higher compressive strength absolutely than other experimental mixes [21]. The parameters that are identified to influence the strength gain process of GPC includes type of binder, binder to AAS ratio, alkali activators ratio, curing time, curing temperature, concentration of AAS, and Si/Al ratio in the binder material and activators [22]. the AAS to binder ratio, molarity, NaOH content, curing temperature, and ages were those parameters that have significant influences on the Compression strength of GPC incorporated with NS [23]. Increasing the molarity and Alkaline to Binder ratios results in the strength development of GPC up to a specific limit [24]. The activation of GBFS with alkaline liquids (e.g., NaOH or water glass) to produce alkali-activated GBFS cement has been studied during the past few decades [25]. GBFS has latent hydraulic properties that could be activated using suitable activators [26]. Metakaolin, fly ash, and mostly GBFS are traditionally used in the production of geopolymer [11]. in GPC, GBFS were used as binder material, along with sodium hydroxide and sodium silicate solutions as AASs [13]. Recent efforts have been made to incorporate various nanomaterials, most notably NS, into GPC to improve the composite's properties [20]. the addition of nanoparticles has a promising future for developing high-performance geopolymer composites that the construction industry can efficiently implement due to significant improvements in strength, durability, microstructure by providing additional C-S-H, N-A-S-H, and C-A-S-H gels as well as filling nano-pores in the geopolymer matrix [8]. the presence of

¹ United Nations

² Environmental, Social, and Governance

nanomaterials, which enhances the rate of polymerization, leads to better performance of the geopolymer [27]. The presence of NS in GPC not only has a positive effect on its physical and mechanical properties but also accelerates the geopolymer reaction, reduces the system's alkalinity, and thus, lowers the degradation of the used fibers [28]. The simultaneous evaluation of NS and steel fibers in GPC has indicated a good relationship between them [29,30]. In an investigation on the effect of POFs with different diameters and lengths in GPCs, it was revealed that the proper use of fibers increases the compressive strength and modulus of elasticity. Besides, adding fibers decreases the compressive strength [31]. In an investigation conducted on the effect of adding 0.5 of POFs to the GPCs, it was observed that the compressive resistance of the samples declined by 12-15%. The samples containing fibers with 55 mm in length had undergone lower compressive strength more than those with 48 mm in length [32,33]. The reason for the reduction in the compressive strength of specimens containing POFs can be the micro internal defects in the geopolymer matrix caused by the additional fibers [34]. Improved elastic modulus have been reported with the use of NS in GPC [35]. The impact of fiber on the long-term behavior of GPC have been highlighted [15]. The addition of different fibers also has essential potential for increasing the performances of geopolymer composites [36]. In addition to the environmental benefits of geopolymers, it possesses excellent mechanical properties, including good resistance to elevated temperatures [17]. Although a novel inorganic family of GPC is a promising building material. The need for understanding its resistance against fire at high temperatures is considered essential to ensure its long-term durability [37]. Physical examinations of the degree of cracking, spalling, brittleness, and loss of strength in GPC upon exposure to high temperatures and during fires provide an indicator of their resilience to such conditions [37]. This structure (related to the GPC) has some merits compared to the regular concrete, e.g., it provides better resistance performance at higher temperatures [38]. The concrete resistance performance against heat is complicated. When being exposed to a high temperature, GPC experiences a number of changes indicated based on their thermal ranges [39].

1. The removal of evaporative water at 100 °C

2. Calcium Silicate Hydrates hydration starts at 180 °C; as the temperature increases to 200 °C, the vapor pressure continuously elevates in the geopolymer structure.

3. The OH hydroxyl groups are evaporated at 500 °C. The dihydroxylation changes the Aluminosilicate structure, reducing the resistance level.

4. An intensely porous ceramic structure is formed at 800 °C.

increase in resistance is observed between room temperature and 200 °C and even 300 °C in research of other researchers, and various reasons are attributed to this increase. For instance, Sadighi et al. in 2012 [40] attributed this increase to the quick-drying of concrete. Similar reports are also provided [41,42]. The effect of NS on improving and reducing heat resistance can be explained as a multi-step mechanism that improves the microstructure of concrete and, consequently, increases the mechanical properties of concrete.

1- Increase in pozzolanic reaction [28]: Presence of NS in GPC increases the rate of pozzolanic reaction.

2- Filers effect of NS particles [43,44]. In the first step, the distribution of the NS particles besides other particles in concrete leads to the creation of a more compact matrix. Secondly, NS reaction in the geopolymerization process produces a greater amount of Aluminosilicate gels and reaction products from main materials.

3- Acting as a nucleus [45,46] In the structure of C-S-H gel, nanoparticles can act as a nucleus and create strong bonds with particles of C-S-H gel. In this laboratory study, increasing the mechanical properties of GBFS geopolymer concrete containing NS and POFs is one of the innovative goals. On the other hand, according to the research of others, helping the healthy environment by reducing CO₂ emissions from conventional cement production, is another goal in this research.

2. Experimental program

2.1. Materials

In this experimental study, the Portland cement type II with a 2.35 g/cm³ of specific weight according to standard En 197-1 and the GBFS was used in powder form with the density of 2.79 g/cm³ according to ASTM C989/C989M standard. The chemical properties of these materials are indicated in Table 1. The NS particles made up of 99.5% SiO₂ with an

average diameter in the range of 15 to 25 nm were used. Crimped POFs according to ASTM D7508/D7508M standard, 30 mm in length, were also used, whose physical properties are shown in Fig. 1. The used fine aggregates (FAs) were natural clean sand with a fineness modulus of 2.95 and a density of 2.75 g/cm^3 , and the coarse aggregates (CAs) were crushed gravel with a maximum size of 19 mm and a density of 2.65 g/cm^3 according to the requirements of the ASTM-C33. In this study, the GPC curing has been performed at 60°C according to the GPC standards extracted from prestigious articles in this field.

Table1

Chemical Compositions of Materials

Component	GBFS (%)	Portland Cement Type II (%)
SiO ₂ (%)	29.2	21.3
Al ₂ O ₃ (%)	19.4	4.7
Fe ₂ O ₃ (%)	5.8	4.3
CaO (%)	38.6	62.7
MgO (%)	2.8	2.1
SO ₃ (%)	2.6	2
K ₂ O (%)	0.1	0.65
Na ₂ O (%)	0.2	0.18
TiO ₂ (%)	0.6	-
Free Cao	-	1.12
LOI (%)	0.3	1.84

2.2. Mix Design

For accurate investigation, six mixture designs were considered, according to ACI 211.1-89 standard. The first sample included a regular concrete containing Portland cement where the water to cement ratio has considered to be constantly 0.45. Five other samples include GPC with different NS and POFs. The GPC samples are generally categorized into two groups: the first group lacks POFs with the NS amount of 0-8%. The second group contains 8% of NS, where the POFs are used in these designs in the form of 1 and 2 percent. In order to achieve the same performance in each mixture design and obtain a slump of about $20 \pm 100 \text{ mm}$, we have used normal polycarboxylate-based superplasticizers. Besides, 202.5 kg/m^3 of the AAS is used in this case. The used AAS is a combination of NaOH and Na₂SiO₃ with the weight ratio of 2.5, utilized with the mixture specific weight of 1483 kg/m^3 and the concentration of 12 M. The conducted studies indicate that due to the significant level of C-S-H formation when utilizing Na₂SiO₃, using a combination of NaOH and Na₂SiO₃ increases the compressive strength compared to single employment of CaOH [47]. The samples mixture design is indicated in Table 2.


Tensile Strength (N/mm ²)	>500	
Length (mm)	30	
Diameter (mm)	0.8	
Elasticity Modulus (GPa)	>11	
Bulk Density(g/cm ³)	2400	

Fig. 1. Physical properties of the POFs

Table 2

Details of the mix designs (kg/m³)

Mix ID	Cement	GBFS	Water	AAS	NS	CAs	FAs	POFs	SP
OPCC	450	0	202.5	0	0	1000	761	0	6.75
GPCNS0POF0	0	450	0	202.5	0	1000	816	0	6.75
GPCNS4POF0	0	432	0	202.5	18	1000	767	0	7.8
GPCNS8POF0	0	414	0	202.5	36	1000	718	0	8.3
GPCNS8POF1	0	432	0	202.5	36	1000	672	24	8.6
GPCNS8POF2	0	432	0	202.5	36	1000	646	48	9

2.3. Test Methods

After fabricating the samples, for better curing and increasing the resistance properties, the samples were placed in an oven at 80 °C with a thermal rate of 4.4 °C/min for 48 h. After taking them out of the oven, the samples were kept for 90 days at an ambient temperature. After curing the samples and before performing the tests heating under standard ISO834, the samples were placed in an oven at 500 °C for 1 h. In the end, by opening the oven door, the samples reached the ambient temperature [48]. In the following, the required experiments were conducted on the concrete samples, according to the related standards. In this study, the compressive strength tests were performed on 10-cm³ cubic specimens based on BS EN 12390. Modulus of elasticity test according to ASTM C469 standard was performed on cylindrical specimens (15 cm in diameter and 30 cm in length). Weight loss test of concrete samples according to ASTM C1792-14 standard was performed on 10 cm³ cubic samples.

3. Results and Discussion

3.1. Results of the Modulus of Elasticity Test

The results of the modulus of elasticity test of concrete samples at 20°C and 500°C temperature are shown in Figure 2. Figure 3 shows the concrete sample after the modulus of elasticity test. The minimum and maximum modulus of elasticity obtained from the samples of control concrete and GPC at a temperature of 500 °C belong to OPCC and GPCNS8POF2 at 13.3 and 28.01 GPa, respectively, this increase in strength by approximately 1.1 times for the design. GPCNS8POF1 contains GPC compared to conventional concrete design. Increasing the fibers in GPCNS8POF1 and GPCNS8POF2 mixing designs, compared to GPCNS8POF0 GPC design, has increased the modulus of elasticity as expected. The maximum increase in modulus of elasticity belongs to the GPCNS8POF2 design, which is 38% more than the 2-GPC design. The maximum and minimum modulus of elasticity of the obtained 90-day concrete sample after heating compared to 90-day concrete samples at room temperature belong to OPCC design and GPCNS8POF1 design by 59% and 32%, respectively. It is generally reported that GPCs that are cured at high temperatures have a lower modulus of elasticity than normal concrete. For each GPC design, we see an increase in the modulus of

elasticity in concrete with increasing consumption of NS and fibers. The highest and lowest percentages of reduction in modulus of elasticity of heat-treated concrete belong to OPCC and GPCNS8POF1 at 59 and 32%, respectively.

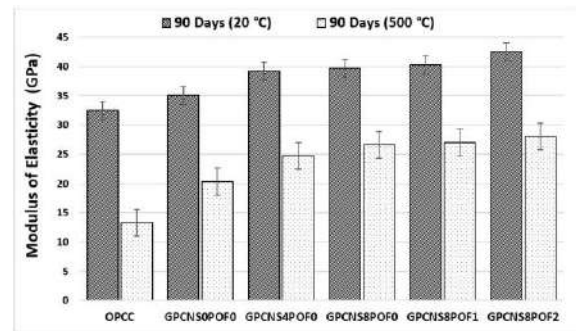


Fig. 2. The Modulus of Elasticity of the specimens



Fig. 3. Modulus of Elasticity Test

3.2. Results of the Compressive Strength Test

The results of the compressive strength test of concrete samples at 20 °C and 500 °C temperature are shown in Figure 4. Figure 5 shows the concrete sample after the compressive strength test.

The minimum and maximum compressive strengths obtained from the samples of control concrete and GPC after exposure to 500 °C belong to OPCC and GPCNS8POF0 designs of 38.89 and 75.99 MPa, respectively. GPCNS8POF0 is approximately 95% warmer than OPCC design. Increasing the fibers in

GPCNS8POF1 and GPCNS8POF2 mixing designs, compared to GPCNS8POF0 GPC design, increases the heat resistance of the sample. Has not been. The maximum and minimum compressive strength of the 90-day samples after heating compared to the 90-day concrete samples at room temperature belong to OPCC design and GPCNS8POF0 design by 37% and 8%, respectively. The percentage of reduction in compressive strength (under high temperature), the effect of the properties of the base materials (GBFS and NS) constituting the GPC in the samples of GPC are evident in the results of the diagram. In this regard, the highest and lowest percentages of reduction in compressive strength of concrete samples belong to the design of OPCC and GPCNS8POF2 by 37 and 8%, respectively.

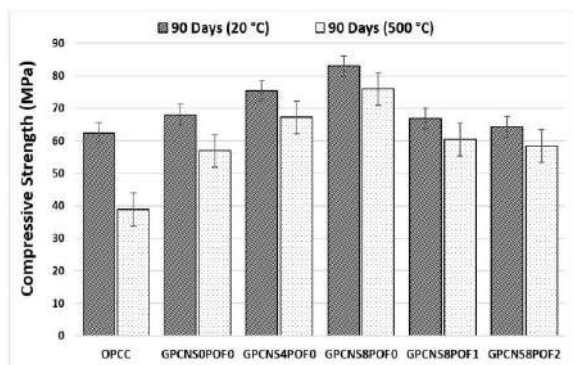


Fig. 4. The Compressive Strength of the Specimens



Fig. 5. Compressive Strength Test

3.3. Results of the weight loss test

The results of the weight loss test of concrete samples at 500 °C temperature are shown in Figure 6. Heat causes water to evaporate and leave the pores, cavities, interlayer and interfacial capillary spaces in the concrete structure and thus affects the weight of the concrete sample, so higher density in the cement matrix structure can be of great help. Maintain the weight of the concrete sample. The lowest weight loss for the sample before and after exposure, the GPCNS8POF0 design shows a 15% improvement in the weight loss test compared to the conventional concrete sample, but with the increase of POFs to GPC. We see severe weight loss in heat-exposed specimens. Weight loss in GPC samples containing heat-treated POFs is more severe than in conventional concrete samples, so that we see a weight loss of 0.12% for the GPCNS8POF0 design, which reached 0.073% for OPCC. The highest (0.12%) and lowest (0.064%) weight loss percentages belong to GPCNS8POF2 and GPCNS8POF0 designs, respectively. From this it can be concluded that the addition of POFs causes weight loss of concrete under heat.

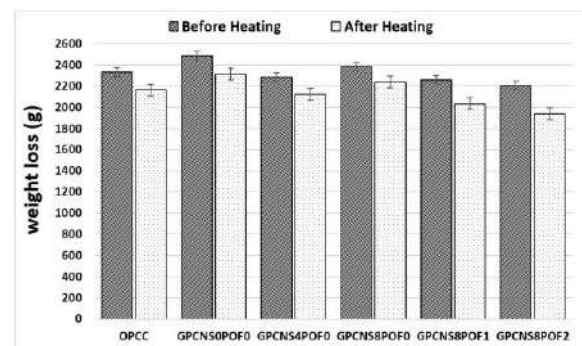


Fig. 6. The Weight Loss of the Specimens

3.4 Results of the SEM Analysis

In this study, SEM at 50 μm and 100 μm scale at 90-day curing age are shown on concrete samples at room temperature in Figure 7 and under high temperature in Figure 8. In the samples at room temperature, in the images obtained from room temperature, it can be seen that designs 2 to 6 include ferrous concrete due to the presence of GBFS and NS, compared to design 1 containing control concrete containing Portland cement of higher density and

cohesion. In their microstructure, this indicates the greater participation of the particles forming ferrous concrete in the geopolymerization process compared to the Portland cement particles in the hydration process.

For ferrous concrete, by increasing the amount of NS in the designs, we see an improvement in the geopolymerization process and an increase in the production volume of hydrated gels in the concrete sample. In Portland cement, C-S-H gel consists of silicone and geopolymer groups of materials with high polymerization and Aluminosilicate structure [49]. In the sample containing NS, very few fine cracks are observed, in which NS acts as a filler to fill the spaces inside the hardened microstructure skeleton of the geopolymer paste and increase its compaction [50,51]. First, the nanoparticles fill the pores of the matrices, which reduces the porosity of the geopolymer nanocomposites, resulting in uniformity, less pores, and a more compact geopolymer matrix [28]. In fact, the pozzolanic reaction condenses and homogenizes the microstructures by converting C-H to C-S-H [52], thus creating more geopolymer gel and a denser matrix [53]. However, further increase in NS content causes insufficient dispersion and accumulation of NS particles, which slightly reduces matrix density [49].

In high temperature samples, tree structure due to water evaporation and destruction of concrete microstructure is observed. In this case, cracks and cavities in the concrete microstructure are seen more than concrete samples under room temperature. For samples after exposure to high temperature, we see evaporation due to evaporation of water evaporated in the microstructure of concrete under the influence of high temperature for all designs. The amount of consumables is less. In general, it is believed that due to their ceramic-like properties, geopolymers have better performance in encountering fire compared to regular concretes [28,54,55].

GPCs resistance in encountering a significant level of heating treatment depends on its constituent chemical compounds and also the temperature and the way of curing [56]. The OH hydroxyl groups are evaporated at 500 °C. The dihydroxylation changes the Aluminosilicate structure, reducing the resistance level [57]. According to the obtained results in this investigation, all designs at room temperature have

"superior" quality, and all samples at 500 °C have average and good quality [58].

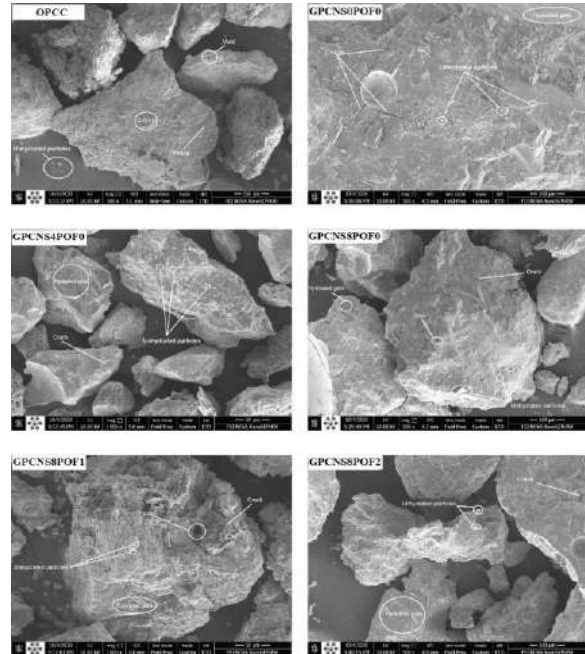


Fig. 7. SEM under room temperature

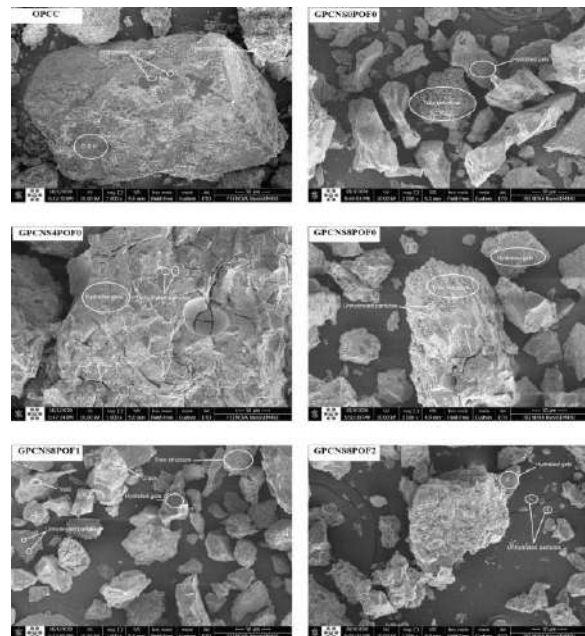


Fig. 8. SEM under high temperature

4. Conclusions

In this experimental study, tensile strength, modulus of elasticity and UPV in OPCC and GPC at 90 days of curing at 20% and 500% were investigated. The results of this research are as follows.

1. At a temperature of 20%, the lowest (32.44 GPa) and highest (42.51 GPa) modulus of elasticity belong to design concrete 1 (including OPCC) and design 6 (including GPC containing 8% NS and 2% POFs). The lowest (62.43 MPa) and the highest (82.96 MPa) compressive strength belong to Scheme 1 (including OPCC) and Scheme 4 (including GPC containing 8% NS).
2. At a temperature of 500%, the lowest (13.3 GPa) and maximum (28.01 GPa) modulus of elasticity belong to design concrete 1 (including OPCC) and design 6 (including GPC containing 8% NS and 2% POFs). The lowest (38.89 MPa) and the highest (75.99 MPa) compressive strength belong to Scheme 1 and Scheme 4 (including GPC containing 8% NS).
3. Applying high heat to GPC samples reduced the modulus of elasticity by up to 42%, compressive strength by up to 16% and reduced the weight of the samples by up to 0.12%. The effect of heat on the drop in results in control concrete is more than GPC.
4. The results of all tests at 20% and 500% showed the superiority of mechanical properties in GPC compared to OPCC.
5. SEM analysis, due to the microstructural superiority of GPC over control concrete, covered the results of other tests in this study.

Credit Authorship Contribution Statement

Mohammadhossein Mansourghanaei:

Conceptualization, Methodology, Validation, Formal analysis, Investigation, Resources, Data curation, Writing - original draft, Writing - review & editing, Visualization, Supervision.

Morteza Biklaryan:

Conceptualization, Formal analysis, Resources, Data curation, Writing - original draft, Writing - review & editing, Visualization, Supervision.

Alireza Mardookhpour:

Conceptualization, Investigation, writing – original draft, Writing - review & editing, Visualization, Supervision.

Declaration of Competing Interest

The authors declare that they have no known competing financial interests or personal relationships that could have appeared to influence the work reported in this paper.

Acknowledgments

This research was done with the support of Islamic Azad University, Chaloos Branch.

Abbreviations

GPC: Geopolymer Concrete
 POFs: Polyolefin Fibers
 GBFS: Granulated Blast Furnace Slag
 NS: Nano Silica (Nano SiO₂)
 OC: Ordinary Concrete
 OPC: Ordinary Portland Cement
 OPCC: Ordinary Portland Cement Concrete
 AAS: Active Alkali Solution
 SEM: Scanning Electron Microscope
 C-H: Calcium-Hydrate
 C-S-H: Calcium-Silicate-Hydrate (C-S-H) or Tobermorite Gel
 C-A-S-H: Calcium-Aluminat- Sulfate-Hydrate (C-A-S-H) or Ettringite Gel or Tobermorite-like gel
 N-A-S-H: Natrium-Aluminat- Sulfate –Hydrate (N-A-S-H) or Tobermorite-like gel
 CAs: Coarse Aggregates
 FAs: Fine Aggregates
 SP: Super Plasticizer
 NaOH: Sodium Hydroxide
 Na₂SiO₃: Sodium silicate
 CaOH: Calcium Hydroxide
 LOI: Loss On Ignition

References

1. Beskopylny, A. N., Shcherban', E. M., Stel'makh, S. A., Mailyan, L. R., Meskhi, B., & El'shaeva, D. (2022). The Influence of Composition and Recipe Dosage on the Strength Characteristics of New Geopolymer Concrete with the Use of Stone Flour. *Applied Sciences*, 12(2), 613.
2. Sathish Kumar, V., Ganesan, N., Indira, P. V., Murali, G., & Vatin, N. I. (2022). Flexural Behaviour of Hybrid Fibre-Reinforced Ternary Blend Geopolymer Concrete Beams. *Sustainability*, 14(10), 5954.

3. Verma, M., Dev, N., Rahman, I., Nigam, M., Ahmed, M., & Mallick, J. (2022). Geopolymer Concrete: A Material for Sustainable Development in Indian Construction Industries. *Crystals*, 12(4), 514.
4. Thakur, M., & Bawa, S. (2022). Self-Compacting geopolymer Concrete: A review. *Materials Today: Proceedings*.
5. Wong, L. S. (2022). Durability performance of geopolymer concrete: A review. *Polymers*, 14(5), 868.
6. Fang, H., & Visintin, P. (2022). Structural performance of geopolymer-concrete-filled steel tube members subjected to compression and bending. *Journal of Constructional Steel Research*, 188, 107026.
7. Srividya, T., PR, K. R., Sivasakthi, M., Sujitha, A., & Jeyalakshmi, R. (2022). A state-of-the-art on development of geopolymer concrete and its field applications. *Case Studies in Construction Materials*, 16, e00812.
8. Ahmed, H. U., Mohammed, A. A., & Mohammed, A. S. (2022). The role of nanomaterials in geopolymer concrete composites: A state-of-the-art review. *Journal of Building Engineering*, 49, 104062.
9. Ahmad, A., Ahmad, W., Aslam, F., & Joyklad, P. (2022). Compressive strength prediction of fly ash-based geopolymer concrete via advanced machine learning techniques. *Case Studies in Construction Materials*, 16, e00840.
10. Asadi, I., Baghban, M. H., Hashemi, M., Izadyar, N., & Sajadi, B. (2022). Phase change materials incorporated into geopolymer concrete for enhancing energy efficiency and sustainability of buildings: a review. *Case Studies in Construction Materials*, e01162.
11. Memiş, S., & Bilal, M. A. M. (2022). Taguchi optimization of geopolymer concrete produced with rice husk ash and ceramic dust. *Environmental Science and Pollution Research*, 29(11), 15876-15895.
12. Jindal, B. B., Alomayri, T., Hasan, A., & Kaze, C. R. (2022). Geopolymer concrete with metakaolin for sustainability: a comprehensive review on raw material's properties, synthesis, performance, and potential application. *Environmental Science and Pollution Research*, 1-26.
13. Kanagaraj, B., Anand, N., Alengaram, U. J., Raj, R. S., & Kiran, T. (2022). Exemplification of sustainable sodium silicate waste sediments as coarse aggregates in the performance evaluation of geopolymer concrete. *Construction and Building Materials*, 330, 127135.
14. Verma, M., & Dev, N. (2022). Effect of liquid to binder ratio and curing temperature on the engineering properties of the geopolymer concrete. *Silicon*, 14(4), 1743-1757.
15. Li, W., Shumuye, E. D., Shiying, T., Wang, Z., & Zerfu, K. (2022). Eco-friendly fibre reinforced geopolymer concrete: A critical review on the microstructure and long-term durability properties. *Case Studies in Construction Materials*, e00894.
16. da Silva, A. C. R., Almeida, B. M., Lucas, M. M., Candido, V. S., da Cruz, K. S. P., Oliveira, M. S., ... & Monteiro, S. N. (2022). Fatigue behavior of steel fiber reinforced geopolymer concrete. *Case Studies in Construction Materials*, 16, e00829.
17. Albidah, A., Alqarni, A. S., Abbas, H., Almusallam, T., & Al-Salloum, Y. (2022). Behavior of Metakaolin-Based geopolymer concrete at ambient and elevated temperatures. *Construction and Building Materials*, 317, 125910.
18. Thomas, B. S., Yang, J., Bahurudeen, A., Chinnu, S. N., Abdalla, J. A., Hawileh, R. A., ... & Hamada, H. M. (2022). Geopolymer concrete incorporating recycled aggregates: A comprehensive review. *Cleaner Materials*, 100056.
19. Lyu, X., Robinson, N., Elchalakani, M., Johns, M. L., Dong, M., & Nie, S. (2022). Sea sand seawater geopolymer concrete. *Journal of Building Engineering*, 50, 104141.
20. Ahmed, H. U., Mohammed, A. S., Faraj, R. H., Qaidi, S. M., & Mohammed, A. A. (2022). Compressive strength of geopolymer concrete modified with nano-silica: Experimental and modeling investigations. *Case Studies in Construction Materials*, 16, e01036.

21. Amin, M., Elsakhawy, Y., Abu el-hassan, K., & Abdelsalam, B. A. (2022). Behavior evaluation of sustainable high strength geopolymers concrete based on fly ash, metakaolin, and slag. *Case Studies in Construction Materials*, 16, e00976.
22. Upadhyay, H., Mungule, M., & Iyer, K. K. (2022). Issues and challenges for development of geopolymer concrete. *Materials Today: Proceedings*.
23. Ahmed, H. U., Mohammed, A. S., & Mohammed, A. A. (2022). Proposing several model techniques including ANN and M5P-tree to predict the compressive strength of geopolymer concretes incorporated with nano-silica. *Environmental Science and Pollution Research*, 1-25.
24. Shilar, F. A., Ganachari, S. V., Patil, V. B., Khan, T. Y., & Dawood, S. (2022). Molarity activity effect on mechanical and microstructure properties of geopolymer concrete: A review. *Case Studies in Construction Materials*, e01014.
25. Allahverdi, A. L. I., Kani, E. N., & Yazdanipour, M. (2011). Effects of blast-furnace slag on natural pozzolan-based geopolymer cement. *Ceramics-Silikáty*, 55(1), 68-78.
26. Davidovits J.: US Patent No. 4509985, 1985.
27. Shilar, F. A., Ganachari, S. V., Patil, V. B., Khan, T. Y., Almakayeel, N. M., & Alghamdi, S. (2022). Review on the relationship between nano modifications of geopolymer concrete and their structural characteristics. *Polymers*, 14(7), 1421.
28. Assaedi, H., Alomayri, T., Shaikh, F., & Low, I. M. (2019). Influence of nano silica particles on durability of flax fabric reinforced geopolymer composites. *Materials*, 12(9), 1459.
29. Gülşan, M. E., Alzebaree, R., Rasheed, A. A., Niş, A., & Kurtoglu, A. E. (2019). Development of fly ash/slag based self-compacting geopolymer concrete using nano-silica and steel fiber. *Construction and Building Materials*, 211, 271-283.
30. Their, J. M., & Özakça, M. (2018). Developing geopolymer concrete by using cold-bonded fly ash aggregate, nano-silica, and steel fiber. *Construction and Building Materials*, 180, 12-22.
31. Rashad, A. M. (2019). The effect of polypropylene, polyvinyl-alcohol, carbon and glass fibres on geopolymers properties. *Materials Science and Technology*, 35(2), 127-146.
32. Noushini, A., Castel, A., & Gilbert, R. I. (2019). Creep and shrinkage of synthetic fibre-reinforced geopolymer concrete. *Magazine of Concrete Research*, 71(20), 1070-1082.
33. Noushini, A., Hastings, M., Castel, A., & Aslani, F. (2018). Mechanical and flexural performance of synthetic fibre reinforced geopolymer concrete. *Construction and Building Materials*, 186, 454-475.
34. Wang, K., Shah, S. P., & Phuaksuk, P. (2002). Plastic shrinkage cracking in concrete materials-Influence of fly ash and fibers. *ACI Materials Journal*, 99(5), 512-513.
35. Ekinici, E., Türkmen, İ., Kantarci, F., & Karakoç, M. B. (2019). The improvement of mechanical, physical and durability characteristics of volcanic tuff based geopolymer concrete by using nano silica, micro silica and Styrene-Butadiene Latex additives at different ratios. *Construction and Building Materials*, 201, 257-267.
36. Kuranlı, Ö. F., Uysal, M., Abbas, M. T., Cosgun, T., Niş, A., Aygörmüş, Y., ... & Al-mashhadani, M. M. (2022). Evaluation of slag/fly ash based geopolymer concrete with steel, polypropylene and polyamide fibers. *Construction and Building Materials*, 325, 126747.
37. Amran, M., Huang, S. S., Debbarma, S., & Rashid, R. S. (2022). Fire resistance of geopolymer concrete: A critical review. *Construction and Building Materials*, 324, 126722.
38. Aslani, F. (2016). Thermal performance modeling of geopolymer concrete. *Journal of Materials in Civil Engineering*, 28(1), 04015062.
39. Bakhtiyari, S., Allahverdi, A., Rais-Ghasemi, M., Zarrabi, B. A., & Parhizkar, T. (2011). Self-compacting concrete containing different powders at elevated temperatures-Mechanical properties and changes in the phase

- composition of the paste. *Thermochimica acta*, 514(1-2), 74-81.
40. Zhuang, X. Y., Chen, L., Komarneni, S., Zhou, C. H., Tong, D. S., Yang, H. M., ... & Wang, H. (2016). Fly ash-based geopolymer: clean production, properties and applications. *Journal of Cleaner Production*, 125, 253-267.
 41. Zhang, B., & Bicanic, N. (2002). Residual fracture toughness of normal-and high-strength gravel concrete after heating to 600 C. *Materials Journal*, 99(3), 217-226.
 42. Fan, F., Liu, Z., Xu, G., Peng, H., & Cai, C. S. (2018). Mechanical and thermal properties of fly ash based geopolymers. *Construction and Building Materials*, 160, 66-81.
 43. Beigi, M. H., Berenjian, J., Omran, O. L., Nik, A. S., & Nikbin, I. M. (2013). An experimental survey on combined effects of fibers and nanosilica on the mechanical, rheological, and durability properties of self-compacting concrete. *Materials & Design*, 50, 1019-1029.
 44. Deb, P. S., Sarker, P. K., & Barbhuiya, S. (2016). Sorptivity and acid resistance of ambient-cured geopolymer mortars containing nano-silica. *Cement and Concrete Composites*, 72, 235-245.
 45. Bahadori, H., & Hosseini, P. (2012). Reduction of cement consumption by the aid of silica nanoparticles (investigation on concrete properties). *Journal of Civil Engineering and Management*, 18(3), 416-425.
 46. Bosiljkov, V. B. (2003). SCC mixes with poorly graded aggregate and high volume of limestone filler. *Cement and Concrete Research*, 33(9), 1279-1286.
 47. Pilehvar, S., Cao, V. D., Szczotok, A. M., Carmona, M., Valentini, L., Lanzón, M., ... & Kjøniksen, A. L. (2018). Physical and mechanical properties of fly ash and slag geopolymer concrete containing different types of micro-encapsulated phase change materials. *Construction and Building Materials*, 173, 28-39.
 48. Kong, D. L., & Sanjayan, J. G. (2010). Effect of elevated temperatures on geopolymer paste, mortar and concrete. *Cement and concrete research*, 40(2), 334-339.
 49. Supit, S. W. M., & Shaikh, F. U. A. (2015). Durability properties of high volume fly ash concrete containing nano-silica. *Materials and structures*, 48(8), 2431-2445.
 50. Deb, P. S., Sarker, P. K., & Barbhuiya, S. (2015). Effects of nano-silica on the strength development of geopolymer cured at room temperature. *Construction and building materials*, 101, 675-683.
 51. Shih, J. Y., Chang, T. P., & Hsiao, T. C. (2006). Effect of nanosilica on characterization of Portland cement composite. *Materials Science and Engineering: A*, 424(1-2), 266-274.
 52. Du, H., Du, S., & Liu, X. (2014). Durability performances of concrete with nano-silica. *Construction and building materials*, 73, 705-712.
 53. Phoo-ngernkham, T., Chindaprasirt, P., Sata, V., Hanjitsuwan, S., & Hatanaka, S. (2014). The effect of adding nano-SiO₂ and nano-Al₂O₃ on properties of high calcium fly ash geopolymer cured at ambient temperature. *Materials & Design*, 55, 58-65.
 54. Ryu, G. S., Lee, Y. B., Koh, K. T., & Chung, Y. S. (2013). The mechanical properties of fly ash-based geopolymer concrete with alkaline activators. *Construction and building materials*, 47, 409-418.
 55. Mehdipour, S., Nikbin, I. M., Dezhampanah, S., Mohebbi, R., Moghadam, H., Charkhtab, S., & Moradi, A. (2020). Mechanical properties, durability and environmental evaluation of rubberized concrete incorporating steel fiber and metakaolin at elevated temperatures. *Journal of Cleaner Production*, 254, 120126.
 56. Türkmen, İ., Maraş, M. M., Karakoç, M. B., Demirboğa, R., & Kantarci, F. (2013, October). Fire resistance of geopolymer concrete produced from Ferrochrome slag by alkali activation method. In *2013 International Conference on Renewable Energy Research and Applications (ICRERA)* (pp. 58-63). IEEE.
 57. Kong, D. L., & Sanjayan, J. G. (2010). Effect of elevated temperatures on geopolymer paste, mortar and concrete. *Cement and concrete research*, 40(2), 334-339.
 58. Whitehurst, E. A. (1951, February). Soniscope tests concrete structures. In *Journal Proceedings* (Vol. 47, No. 2, pp. 433-444).



Comparative study of numerical methods used in prediction of post-crack behavior of waffle slabs

Alireza Sheikhnasiri ^{a*}

^aPh.D Student, Structural Orientation, Faculty of Islamic Azad University, (Chalous Branch), Mazandaran, Chalous, Iran

Journals-Researchers use only: Received date: 2022.10.23; revised date: 2022.11.16; accepted date: 2022.11.21

Abstract

One effective way to reduce dead and earthquake loads is to use waffle slabs. The use of waffle slabs leads to smaller sections. There are various methods for predicting the behavior of slabs, the most important of which is fracture mechanics. Considering the variety of geometry of waffle slabs, it is important to investigate the formation and growth of cracks in them. The current research aims to analyze the post-crack behavior of waffle slabs under common loading conditions using the finite element method by using numerical modeling to analyze cracks in reinforced concrete members. by comparing the obtained results with the laboratory sample, the optimal numerical model for predicting the behavior of the hollow slab was determined. The waffle slab sample was modeled with two types of distributed and concentrated loading conditions and two types of simple and fixed support conditions. The models were modeled by two methods of concrete damage plasticity and smeared cracked concrete by Abaqus software. Various parameters of these samples, including the load-displacement diagram, the load coincident with the formation of cracks, the displacement in the middle of the slab opening, and the pattern of the formation and propagation of cracks, etc., were discussed and investigated. To validate and control the modeling process, the laboratory results of the research of Nithyambigai G et al. in 2021 have been used. The outcomes of this study showed; a relatively good correspondence between the two methods of Concrete damage plasticity and the concrete smeared crack model, but due to the definition of failure in the Concrete damage plasticity method, more accurate results can be obtained. © 2017 Journals-Researchers. All rights reserved (DOI:<https://doi.org/10.52547/JCER.4.4.12>)

"Keywords: CDP Numerical Method, Crack Growth, Reinforced Concrete Slab, Concrete Smeared Cracking Method, waffle Slab."

1. Introduction

The most significant challenge for engineers in analyzing the behavior of reinforced concrete members is to predict how cracks will form and propagate in them. Also, the effect of the formation

of cracks on various components such as hardness, load, deformations, and durability in reinforced concrete members is important. one of the important components of structures that are responsible for carrying a major part of the load on the structure is slabs. Methods such as finite element analysis are used to predict the formation and expansion of cracks in reinforced concrete members like slabs. Abaqus is one of the software for finite element modeling and

* Corresponding author. Tel.: +989904417166; e-mail: Alireza.sa30@gmail.com

analysis. This software can simulate reinforced concrete members.

Classical models for concrete cracking are based either on the so-called smeared crack approach or the discrete crack approach. Smeared crack models are based on the theory of continuum mechanics and are characterized by spreading the dissipated energy along the width of the localization band. The class of discrete crack models is characterized by incorporating the discontinuity of the displacement field due to cracking directly into the finite element formulation to capture the strong discontinuity kinematics of a discrete crack.[1] In the early days of finite elements, analysis cracks were modeled using separation between element edges (Ngo and Scordelis 1967, Nilson 1968). The approach suffers from two drawbacks. First, it implies a continuous change in nodal connectivity, which does not fit the nature of the finite element displacement method. Secondly, the crack is constrained to follow a predefined path along the element edges. The counterpart of the discrete crack concept is the smeared crack concept, in which a cracked solid is imagined to be a continuum. The approach introduced by Rashid (1968) starts from the notion of stress and strain and permits a description in terms of the stress-strain relation. This approach preserves the topology of the original finite element mesh and does not impose restrictions concerning the orientation of crack planes.[2]

Bangash (1989) has provided a step-by-step definition for modeling cracks from their formation and propagation to opening and closing under stepwise loading. In this definition, where the cracks are formed, the tensile stress cannot be directly defined in the direction perpendicular to the cracks. A concrete element parallel to the crack is considered to receive stresses defined based on biaxial or triaxial continuity relations in the plane parallel to the crack.[3]

Three methods of concrete damage plasticity, concrete smeared cracking and brittle cracking are used for crack modeling in Abaqus software. The generalized concrete damage plasticity model is the Drucker-Prager failure criterion, and it is one of the strong theories in reinforced concrete failure modeling. The concrete damaged plasticity model assumes nonassociated potential plastic flow. The

flow potential used for this model is the Drucker-Prager hyperbolic function. Drucker Prager's (1952) rupture criterion is a generalized Mohr-Coulomb rupture criterion for all types of soil.[4] The model makes use of the yield function of Lubliner et. al. (1989), with the modifications proposed by Lee and Fenves (1998) to account for different evolution of strength under tension and compression.[5][6] in the concrete smeared cracking method, when there is no reinforcement in significant regions of a concrete model, the strain softening approach for defining tension stiffening may introduce unreasonable mesh sensitivity into the results. Crisfield (1986) discusses this issue and concludes that Hiller Borg's (1976) proposal is adequate to allay the concern for many practical purposes. Hiller Borg defines the energy required to open a unit area of crack as a material parameter, using brittle fracture concepts.[7] With this approach, the concrete's brittle behavior is characterized by a stress-displacement response rather than a stress-strain response. Under tension, a concrete specimen will crack across some sections. After it has been pulled apart sufficiently for most of the stress to be removed (so that the elastic strain is small), its length will be determined primarily by the opening at the crack.

2. Methodology

This research has been done with the ABAQUS finite element software. The background of the work and relevant theories in the field of crack analysis in reinforced concrete sections were studied. The results of valid laboratory studies in the field of waffle slabs were selected and the relevant samples were modeled and analyzed. Using the results obtained from the numerical analysis, the pattern of crack formation and propagation and load-displacement diagram were compared with the laboratory samples. Software analysis is given in two parts. The first part is about validation. To validate the results obtained from Abaqus, they were compared with the laboratory samples of the article (Behavior of waffle slab Nithyambigai G (2021)).[8] In the second part, the crack formation and propagation pattern and the load-displacement diagram of numerical samples under different loading and support conditions were

compared with concrete damage plasticity and concrete smeared cracking methods.

2.1. validation

Five samples of waffle slabs have been investigated in the reference article under the title of hollow slab behavior. The slabs have different

dimensions on a scale of 1 to 5. Samples of waffle slabs have been compared with samples of flat slabs. Concrete with a compressive strength of 47 MPa and a modulus of elasticity of 31877 MPa has been used. Rebars with a yield strength of 400 MPa and ultimate strength of 600 MPa and modulus of elasticity of 200000 MPa were used. Table (1) shows the mentioned values.

Table 1

Concrete mechanical properties

Material type	Compressive strength (MPa)	modulus of elasticity (MPa)	yield strength (MPa)	ultimate strength (MPa)
concrete	47	31877	-	-
rebar	2×10^5	-	400	600

To simulate the compressive stress behavior of concrete in the CDP method, the modified Hognestad (1951) relation has been used.[9] Equations (1) and (2) represent the modified Hognestad.

$$f_c = f_c' \left[2 \left(\frac{\epsilon_c}{\epsilon_{cu}} \right) - \left(\frac{\epsilon_c}{\epsilon_{cu}} \right)^2 \right] \quad \text{for } 0 \leq \epsilon_c < \epsilon_{cu} \quad (1)$$

$$f_c = f_c' [1 - Z(\epsilon_c - \epsilon_{cu})] \quad \text{for } \epsilon_{cu} \leq \epsilon_c < \epsilon_{cu} \quad (2)$$

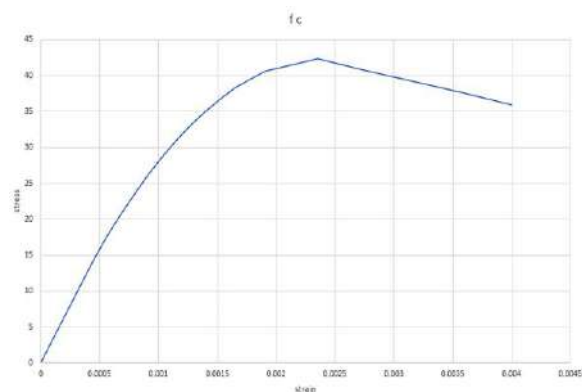


Fig. 1. A Uniaxial compressive stress-strain diagram of concrete

In the upcoming research, the modified model of Wahalathantri Buddhi et.al, (2011) has been used.[10] This model is the modified method of Nayal and Rashid. [11]

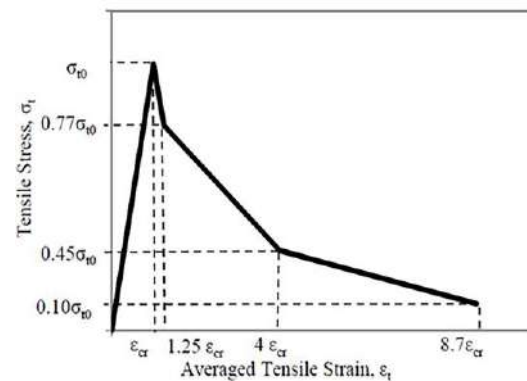


Fig. 2. Wahalathantri tension stiffening model

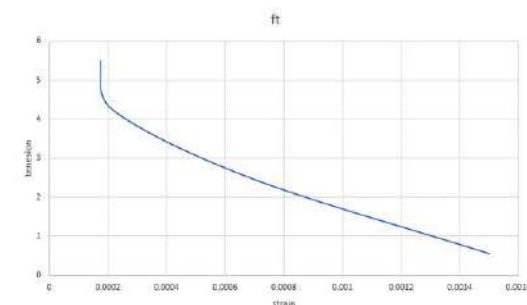


Fig. 3. Uniaxial tensile stress-strain diagram of the sample
The compressive and tensile failure parameter in the CDP method is defined by equation (3).

$$d_c = 1 - \frac{\sigma_c}{f_c} \quad , \quad d_t = 1 - \frac{\sigma_t}{f_t} \quad (3)$$

For the smeared cracking method, the pressure values are the same as the plastic failure. For the concrete-smeared cracking method, the tension stiffening effect must be estimated; it depends on such factors as the density of reinforcement, the quality of the bond between the rebar and the concrete, the relative size of the concrete aggregate compared to the rebar diameter, and the mesh. when there is no reinforcement in significant regions of a concrete model, the strain softening approach for defining tension stiffening may introduce unreasonable mesh sensitivity into the results. Crisfield (1986) discusses this issue and concludes that Hillerborg's (1976) proposal is adequate to allay the concern for many practical purposes. Hillerborg defines the energy required to open a unit area of crack as a material parameter, using brittle fracture concepts. With this approach, the concrete's brittle behavior is characterized by a stress-displacement response rather than a stress-strain response. For linear elements, the amount of displacement is obtained by multiplying the length of the element by the amount of strain coinciding with the crack initiation, which is equal to 5×10^{-5} .

2.2. Modeling

Abaqus finite element analysis software was used for the modeling and analysis of samples. Fig. 4. Shows a waffle slab modeled in Abaqus.

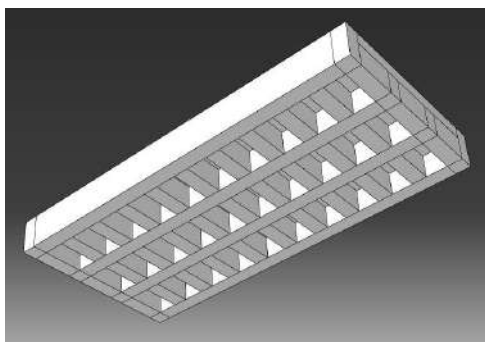


Fig. 4. Schematic view of waffle slab

The waffle slab was modeled with a scale of 1:5 and dimensions of 90 x 500 x 1020 mm. The beam sizes are 60x40mm and were tied in various spacing.

Beams were tied in an interlocking manner as a grid. The reinforcement detailing on the beam in top 1# 6mmØ and bottom 1# 6mmØ. Stirrups for the beam are 30 mm _ 50 mm of 6 mm Ø. The stirrups were placed at a distance of various c-c. The top slab is 30 mm thick and the reinforcing details of 100 mm spacing of 8 mm Ø.

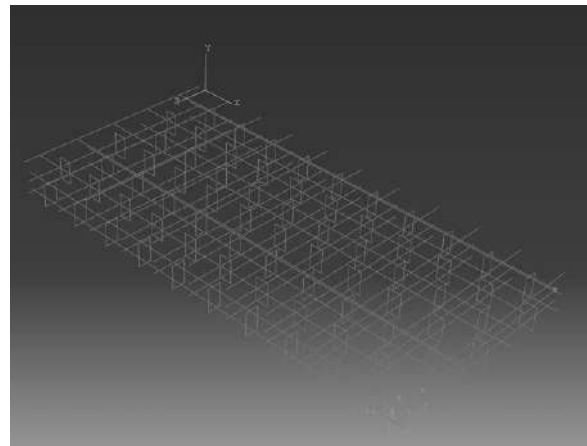


Fig. 5. Schematic view of rebars

The experimental sample has simple supports and the load is concentrated on a 130x130 mm plate. The results of the load- displacement of concrete damage plasticity and concrete smeared cracking are shown in figures (6) and (7).

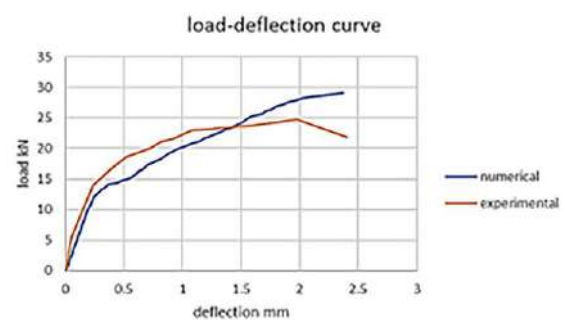


Fig. 6. Comparison of displacement force diagram of concrete damage plasticity model with the experimental sample in concentrated load mode with simple support

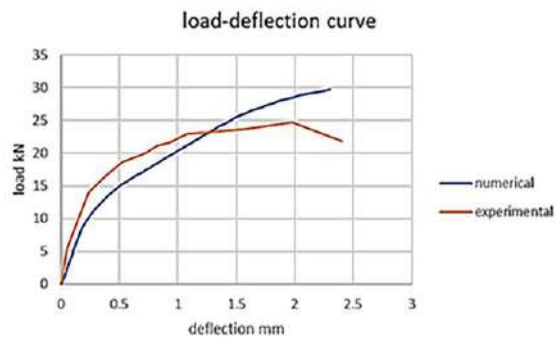


Fig. 7. Comparison of displacement force diagram of concrete smeared cracking model with the experimental sample in concentrated load mode with simple support

By comparing the load-displacement diagram of the experimental and numerical samples, it was determined that there is a good match between them.

2.3. Boundary condition

Two types of boundary conditions were modeled. One is a simple support and the other is a fixed support. Fig.8. and Fig.9.

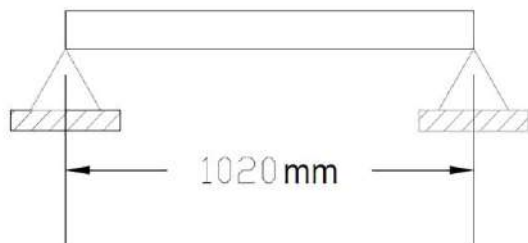


Fig. 8. Simple support condition

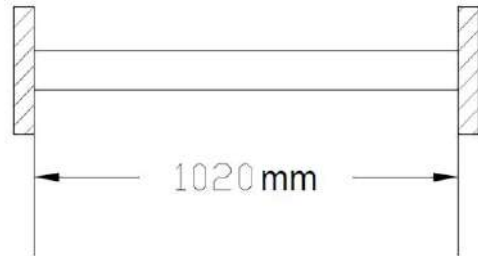


Fig. 9. fixed support condition

2.4. loading

Four types of boundary conditions and different loading are modeled. waffle slab with simple support and concentrated loading, waffle slab with simple support and distributed loading, waffle slab with fixed support and concentrated loading, and waffle slab with fixed support and distributed loading.

In the Specimens with concentrated load, the load is applied as a pressure on a part of the middle of the slab with dimensions of 130x130 square mm. In specimens with a uniform load, the load is applied widely on the upper part of the slab.

3. Results and discussion

The results of the load-displacement diagram of two concrete damage plasticity and concrete smeared cracking methods for the four named specimens are shown in Fig.10. to Fig.13.

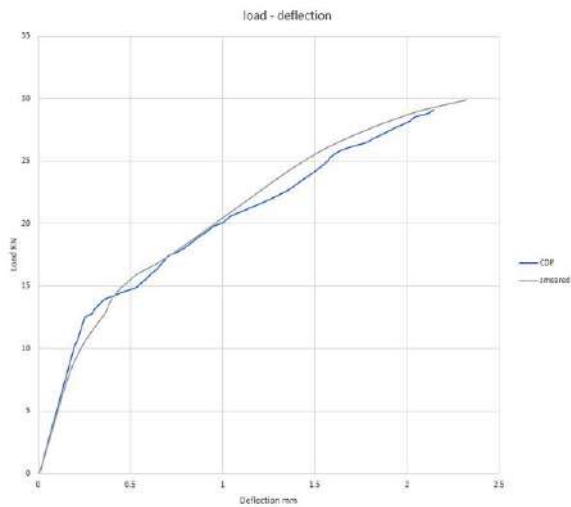


Fig. 10. Comparison of load-displacement of two concrete damage plasticity and concrete smeared cracking methods in case of concentrated load with simple support

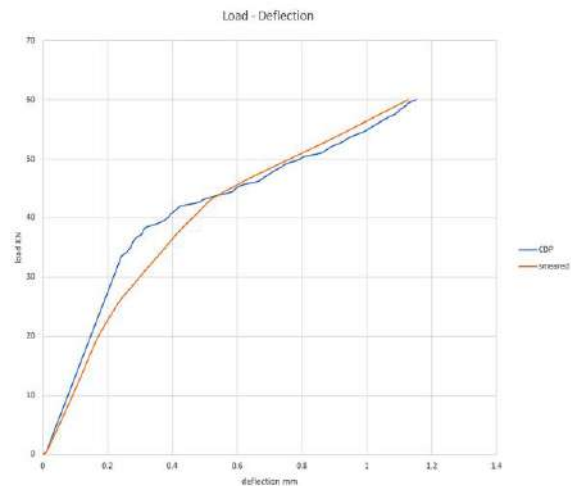


Fig. 11. Comparison of load-displacement of two concrete damage plasticity and concrete smeared cracking methods in case of uniform load with simple support

In the simple supported concentrated load case, both methods are similar up to a loading of 7 KN, but after that, the concrete smeared cracking method is almost trilinear. For the case of uniform load with simple support, the incline of the linear part of the diagram of the concrete damage plasticity model is higher and this linear function continues up to the load of 33.6 KN. However, in the concrete smeared cracking method, the performance is still almost

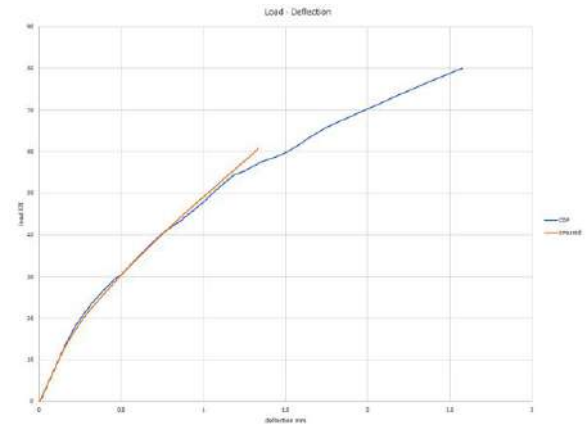


Fig. 12. Comparison of load-displacement of two concrete damage plasticity and concrete smeared cracking methods in case of concentrated load with fixed support

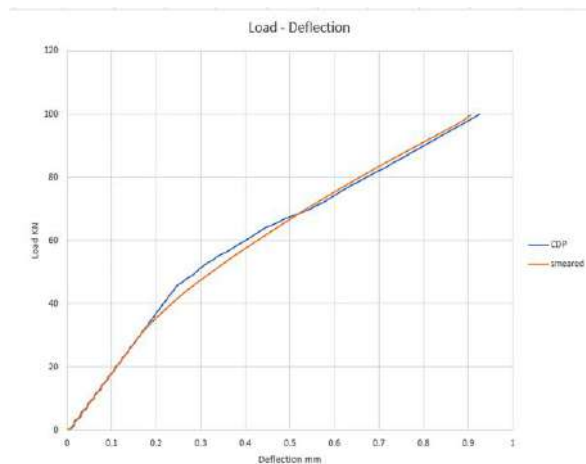


Fig. 13. Comparison of load-displacement of two concrete damage plasticity and concrete smeared cracking methods in case of uniform load with fixed support

three-line, and the incline of the initial part is gentler and has a linear performance up to a load of 19.2 KN. In the case of a concentrated load with fixed support, the two methods are in good agreement with each other, and the incline of the graphs is almost the same. In the concrete damage plasticity method, the loading is linear up to the load value of 18 KN and this value is equal to 15 KN for the concrete smeared cracking method. Due to the problems of convergence in the concrete smeared cracking

method, it was calculated up to 60 KN. For the case of uniform load with fixed supports, the slope of the linear part of the graph of the CDP method is higher and this linear function continues up to a load of 45 KN. The concrete smeared cracking method is still almost three-linear. The incline of the initial part is almost the same as the concrete damage plasticity method and has a linear performance up to a load of 33 KN. In general, the displacement load values of the two methods are in good agreement with each other for all specimens.

For the concrete damage plasticity method, tensile damage is used as a criterion to identify the first crack. The maximum principal plastic strain criterion is used to identify the first crack for the concrete smeared cracking method. The chart comparing the initiation crack load for both methods is given in Fig.14. and Fig.15.

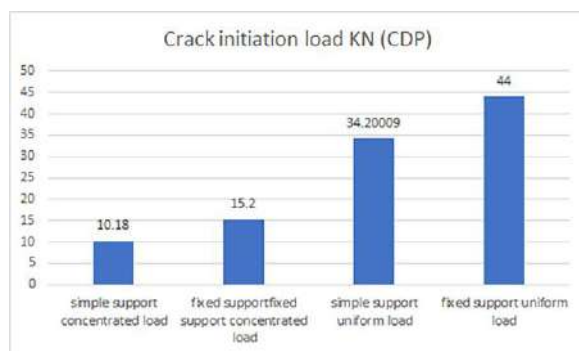


Fig. 14. Initial cracking load for concrete damage plasticity

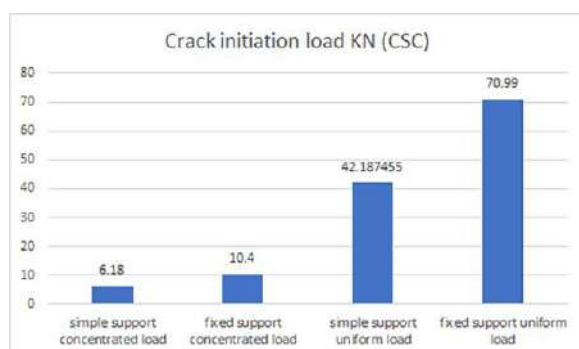


Fig. 15. Initial cracking load for concrete smeared cracking

4. Conclusions

The following points were concluded based on the values obtained from the model.

- The concrete smeared cracking method can only be used for static analysis, and the analysis process based on time increments in this method cannot continue until the end, and eventually, too many attempts made for this increment will be shown. In the concrete smeared cracking method, some specimens did not complete the analysis until the end, which caused less accuracy in the obtained answer.
- The initial crack load for waffle slab with simple support and concentrated loading, waffle slab with fixed support and concentrated loading, waffle slab with simple support and uniform loading, and waffle slab with fixed support and distributed loading, respectively, for concrete damage plasticity model 10.18, 15.2, 34.2, 44 KN has been obtained. And for concrete smeared cracking model 6.18, 10.4, 42.19, and 70.99 KN has been obtained.
- The reason for the huge difference in the initial cracking load in the specimen of fixed support with uniform load is the lack of definition of tensile damage in the concrete smeared cracking method. Because the initial crack in the concrete damage plasticity method was determined using the tensile damage criterion at a load of 44 KN, while in the concrete smeared cracking method, the crack location is determined only through the maximum principal plastic strain.
- The load-displacement diagram of the two methods is almost identical in the linear region, but in the non-linear region, the concrete smeared cracking method is almost trilinear.
- The compatibility of the load-displacement diagram of the two methods is more in the case of fixed support.

References

- [1] Hofstetter Guenter, Meschke Gunther, 2011, Numerical Modeling of Concrete Cracking, Springer Science & Business Media.

- [2] Rots, J.G., Blaauwendraad, J., 1989, Crack Models for Concrete, Discrete or Smeared. Fixed, Multi-Directional or Rotating., Delft University of Technology.
- [3] Bangash. M. Y. H., 1989, Concrete and Concrete structures: Numerical modeling and applications, Elsevier.
- [4] Drucker DC, Prager W, (1952), Soil mechanics and plastic analysis or limit design, Q Appl Math, pp 157–165
- [5] Lubliner, J., J. Oliver, S. Oller, and E. Oñate, “A Plastic-Damage Model for Concrete,” *International Journal of Solids and Structures*, vol. 25, pp. 299–329, 1989.
- [6] Lee, J., and G. L. Fenves, “Plastic-Damage Model for Cyclic Loading of Concrete Structures,” *Journal of Engineering Mechanics*, vol. 124, no.8, pp. 892–900, 1998.
- [7] Hillerborg, A., M. Modeer, and P. E. Petersson, “Analysis of Crack Formation and Crack Growth in Concrete by Means of Fracture Mechanics and Finite Elements,” *Cement and Concrete Research*, vol. 6, pp. 773–782, 1976.
- [8] Niyhyambigai G., Rameshwaran P.M., Stella Mary F., (2021), “Behavior of waffle slab”, Elsevier, Vol 46, No 9, pp 3765-3768
- [9] Hognestad E., (1951), “A Study of Combined Bending and Axial Load in Reinforced Concrete Members”, Bulletin 399, University of Illinois Engineering Experiment Station Urbana, pp 128.
- [10] Wahalathantri Buddhi. L., Thambiratnam David, Chan Tommy, Fawzia Sabrina, (2011), “A Material Model for Flexural Crack Simulation in Reinforced Concrete Elements Using ABAQUS”, First International Conference on Engineering, Designing and Developing the Built Environment for Sustainable Wellbeing, Queensland University of Technology, Australia, pp 260-264
- [11] Nayal, R., Rasheed, H.A. (2006). Tension Stiffening Model for Concrete Beams Reinforced with Steel and FRP Bars. *Journal of Materials in Civil Engineering*, Vol 18, No 6, pp 831-841.



Investigating the compressive and tensile strength of concrete containing recycled aggregate with polypropylene fibers

Donya Khazraie^{a*}, Hossein Razzaghi^a

^aPooyandegan danesh chalous, Chalous, Iran

Journals-Researchers use only: Received date: 2022.10.22; revised date: 2022.11.17; accepted date: 2022.11.20

Abstract

In this research, recycled concrete aggregates were used instead of natural aggregates in concrete, and then the recycled concrete was reinforced with polypropylene fibers. The purpose of this study is to first investigate the effect of replacing recycled aggregates with natural aggregates on the mechanical resistance of concrete and then to investigate the effect of adding polypropylene and micro silica fibers on concrete containing natural and recycled aggregates in two water-to-cement ratios of 0.4 and 0.55. The results of this research show that by replacing recycled aggregates with natural aggregates, the compressive and tensile strengths of concrete have decreased significantly. Also, the results show that the addition of polypropylene fibers with a weight ratio of 1.5% had a significant effect in compensating the reduction of compressive and tensile strengths in recycled concrete. It should be mentioned that the samples containing microsilica and polypropylene fibers in all mixing designs (natural and recycled aggregates) had higher resistance values (tension and pressure) than the samples without microsilica. Also, concrete samples with a water-cement ratio of 0.4 had higher compressive strengths than concrete samples with a water-cement ratio of 0.55. © 2017 Journals-Researchers. All rights reserved. (DOI: <https://doi.org/10.52547/JCER.4.4.20>)

Key words: concrete; recycled aggregates; polypropylene fibers; microsilica; compressive strength.

1. Introduction

In recent years, the use of concrete has grown significantly around the world, and the use of concrete in the construction industry is increasing day by day. With this increasing trend, in the not-so-distant future, we will definitely face a shortage of mineral resources used to prepare natural aggregates, and we must inevitably seek to find a

suitable alternative for natural aggregates [1, 2]. Due to the limitation of the life of concrete structures and the destruction of concrete structures due to natural factors such as earthquakes, floods, storms, etc., we are always faced with a large amount of waste and damaged concrete, whose accumulation in landfills causes many problems for the environment. Life has created [3, 4]. Protecting the environment and preventing the speed of reducing the destruction of natural resources is one of the basic measures in the direction of sustainable

* Corresponding author. Tel.: +098-933-352-5552; e-mail: donya.khazraie@gmail.com.

development. Continuous industrial development will bring serious problems due to the burial of construction waste and destructive concrete. A solution to solve this problem is to use these destructive concretes as recycled concrete aggregates, as a substitute for natural aggregates, to try to preserve the environment in addition to reducing the use of natural resources [5]. Research into the reuse of destroyed concrete and building materials as aggregates for new concrete dates back to the end of World War II. For the first time, the recycling of waste concrete caused by destruction and construction after World War II in Germany was done by Mr. Khalaf and his colleagues. Since then, extensive research work has been done in developed countries on the possibility of reusing recycled concrete in new concrete [6]. According to some studies, the use of recycled aggregates with a replacement percentage of 20-30% does not have a negative effect on the physical and mechanical properties of concrete made from these aggregates [7-11]. On the other hand, if the replacement percentage is 100%, the compressive, tensile and bending strengths of concrete will decrease by 20%, which can be attributed to the heterogeneity of recycled materials [12].

Also, research has shown that by increasing the use of recycled concrete materials (sand) instead of natural materials, the amount of water absorption of samples increases [13]. According to the research done, by increasing the amount of waste concrete aggregates (recycled sand) instead of natural aggregates in new concrete, a decrease in compressive, tensile and bending strength as well as an increase in 24-hour water absorption of concrete is observed [14].

According to the research done by Gomez and his colleagues, concrete that is composed of 100% recycled concrete sand will have more porosity than normal concrete, and from the age of 28 days to 90 days, the porosity of the samples will decrease in both types of concrete, and the amount of this reduction will be higher in recycled concrete [15].

Although the use of recycled concrete aggregates in the production of fresh concrete has an unfavorable effect on the physical and mechanical properties of concrete. The use of fibers in concrete and the production of fiber concrete has made it

possible to create concrete with ductility and higher energy absorption ability and with low cracking development under the load and stresses resulting from shrinkage and heat [16].

Fiber concrete is a cement concrete reinforced with distributed fibers. In fiber concrete, thousands of small fibers are dispersed and randomly mixed in concrete during mixing, and therefore we have improvement of concrete properties in all directions. Fibers help to improve concrete ductility, concrete tensile strength, fatigue resistance, impact resistance and shrinkage cracks [17]. Fiber-reinforced concretes have been expanded because they can increase hardness, bending strength, and tensile strength depending on their type [18].

Steel, polymer, glass and carbon fibers are among the artificial fibers that are used today. Polypropylene is a thermoplastic polymer that is one of the cheapest and most widely used fibers in the concrete industry. These fibers have a high resistance to most corrosive environments, including alkaline, acidic and salty, and this feature, along with low density and moisture absorption, has made it the most widely used polymer fiber used in concrete. Propylene is a derivative of petroleum and is cheaper than other raw materials used for polymerization and formation of synthetic Introduction

fibers. Polypropylene fibers are prepared in the form of a linear polymer through the polymerization of propylene, and it is called PP for short [19].

Protection of the environment and primary resources, lack of depot and disposal of construction waste and the high cost of maintenance of construction waste are important factors to increase the attention of countries in the world in using concrete waste as materials used in concrete production [20].

Therefore, the issue of concrete waste recycling is considered important and necessary from an environmental point of view and according to the mentioned problems and the necessity of using recycled concrete, it will also be necessary to study the changes in the properties of this consumable by using fibers and replacing recycled aggregates. Therefore, the purpose of this study is to investigate the usability of polypropylene fibers in concrete

made from recycled aggregates, which are mainly used in concrete.

2- Research method

In this research, recycled concrete aggregates as fine and coarse aggregates have replaced natural aggregates 100%. Also, polypropylene fibers with volume percentages of 0 and 1.5 have been used in the designs. The concrete mixing plan was made by considering the maximum nominal amount of aggregate of 19 mm for water-cement ratios of 40% and 55%. Table 1 shows the amount of materials used in one cubic meter of concrete for different mixing plans.

Considering that the use of waste materials in concrete will reduce the characteristics of hardened

concrete [21] and the use of pozzolanic minerals such as micro silica can improve some of this reduction [22], In this research, in order to improve the properties of concrete with recycled aggregates, micro silica was used at the rate of 9 percent by weight of cement. Also, super-lubricant has been used to reduce water consumption and ensure the required efficiency of concrete. After making concrete, in order to determine the rheological properties of fresh concrete, slump flow test, to check the mechanical properties of concrete, tests of hardened concrete including compressive and tensile strength were performed on the samples. The complete specifications of the concrete plans made are stated in Table No. 1.

Table 1- Specifications of mixing plans

Water to cement ratio	Design name	Polypropylene	recycled concrete	Sand (4.75 to 19 mm) kg/m ³	sand (0 to 4.75 mm) kg/m ³	Cement kg/m ³	Water kg/m ³	silica fume	super lubricant
40%	Pp0-rc0	0%	0%	1024.6	743.3	360	160	40	1%
	Pp1.5-rc0	1.5%	0%	1024.6	743.3	360	160	40	1%
	Pp0-rc100	0%	100%	925.934	743.3	360	160	40	1%
	Pp1.5-rc100	1.5%	100%	925.934	743.3	360	160	40	1%
55%	Pp0-rc0	0%	0%	1009.125	732.062	350	192.5	0	0.8%
	Pp1.5-rc0	1.5%	0%	1009.125	732.062	350	192.5	0	0.8%
	Pp0-rc100	0%	100%	911.950	732.062	350	192.5	0	0.8%
	Pp1.5-rc100	1.5%	100%	911.950	732.062	350	192.5	0	0.8%

2-1- Consumable materials:

In this research, the materials used in the concrete mixing plan include water, cement, natural and recycled crushed aggregates, polypropylene fibers, super-lubricant and micro-silica, whose general characteristics are as follows:

2-1-1- Cement:

The cement used in this research to make all mixing designs is type 2 portland cement from Neka company. The physical and chemical characteristics of this cement are according to Table 2 and 3:

Table 2- Chemical characteristics of used cement

Cl ⁻	SO ₃	Na ₂ O	K ₂ O	MgO	Al ₂ O ₃	CaO	Fe ₂ O ₃	SiO ₂	chemical mixture
0.008	2.49	0.35	0.64	1.27	4.7	64.35	3.18	19.8	Percentage

Table 3- Physical characteristics of used cement

Density (kg/m ³)	Specific surface (cm ² /gr)	Compressive strength (MPa)
3150	3020	435

gravity and water absorption percentage than recycled aggregates.

2-1-2- Aggregate

Considering that approximately 75% of the volume of concrete is made up of aggregates, to prepare the concrete mixing plan, it is necessary to check the specifications of these materials. In this research, two types of aggregates in the size of sand (0 to 4.75 mm) and sand has been used in two categories: pea (4.75 to 9.5 mm) and almond (9.5 to 19 mm).

The natural aggregates (NA) used in this project were obtained from a company in the Marzanabad. Recycled concrete aggregates (RCA) used in this research were prepared from broken materials from a stone crushing plant around the city of Chalous with a maximum grain size of 19 mm.

Preparation operation and Sieving of recycled aggregate it has been done in the stone crusher of this factory. After crushing recycled concrete by jack and stone crusher machines, the obtained aggregates were granulated after passing through the sieve and complying with the requirements of ASTM C33 regulations and it was used in the design of concrete mixes [23]. The granulation curve of natural and recycled aggregates is according to Figure 1. Figure 1 shows the range of coarse grain, fine grain and natural and recycled aggregate curve. The physical characteristics of natural and recycled aggregates used in this research are also presented in Table 4. According to Table 4, natural aggregates have lower specific

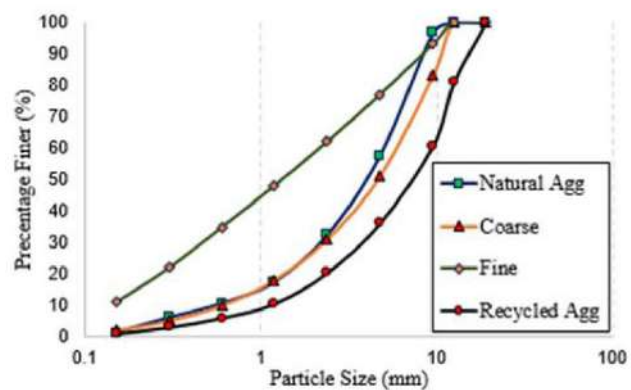


Figure 1- Granulation curve of consumed aggregates (natural and recycled)

2-1-3- Water:

water used to make concrete samples, the drinking water of Chalous city has a specific gravity of 1000 kg/m³, which is suitable for making concrete. The water used in the sample processing pond is non-hard water with 40 grams of lime dissolved per cubic meter.

2-1-4- Consumable fibers (polypropylene):

The fibers used in this research include polypropylene fibers, whose physical and mechanical characteristics are shown in Table 5.

Table 4- Physical characteristics of natural and recycled aggregates

(mm) Aggregate size	Water absorption percentage	(kg/m ³) Density	Materials
6-19	1.5	2720	Natural gravel
6-19	5.5	2620	Recycled gravel
0-6	2.5	2651	Natural sand
0-6	7.5	2230	Recycled sand



Figure 2- Polypropylene fibers used in this research

Table 5- Physical characteristics of polypropylene fibers

0.91	Density (g/cm ³)
18	Length (mm)
0.2	Diameter (mm)
90	Length to diameter ratio (L/D)

This fiber is simple. Figure 2 shows a view of the polypropylene fibers used in this research.

2-1-5- Super lubricant:

In this research, light brown polycarboxylate-based super-lubricant was used to ensure optimal concrete efficiency and reduce water consumption. According to the proposal of its manufacturer, the consumption of this material in concrete is 1 percent by weight of cement, which was used in this research in two ratios of 0.8 and 1 percent.

2-1-6- Micro silica:

Considering that the use of waste materials in concrete will reduce the properties of hardened concrete and the use of pozzolanic minerals such as micro silica can improve some of this reduction. In this research, in order to improve the properties of concrete with recycled aggregate, micro silica was used at the rate of 9 percent by weight of cement [22]. The chemical characteristics of micro silica used in the mixing plans of this research are according to Table No. 6 [37].

2-2- Steps of making and processing concrete samples:

The process of making fiber concrete was similar to concrete without fibers, with the difference that due to the fact that adding fibers requires spending some time, first, the aggregates were added to the mixer within 3 minutes, and the fibers were manually added to the mixture while the mixer was working, and by changing the angle of the mixer and monitoring the mixture, an attempt was made to distribute the fibers evenly in the concrete.

In all stages of concrete making, homogeneous and uniform concrete was made by changing the rotation angle of the mixer axis. After emptying the mixer, the concrete is first turned over with a shovel, and immediately after that, the slump test was performed. According to the measurements, the amount of fresh concrete slump is 10 cm. Also, the temperature of fresh concrete is 27 to 29 degrees Celsius and the temperature of processing water is 20 to 24 degrees Celsius.

Table 6- Chemical characteristics of micro silica

SO ₃	Na ₂ O	MgO	Al ₂ O ₃	CaO	Fe ₂ O ₃	SiO ₂	Chemical mixture
0.19	0.294	0.902	0.748	0.44	0.829	0.19	Percentage

After this stage, concrete was poured into lubricated cubic, cylindrical and prismatic molds and placed in laboratory conditions for 24 hours to harden.

After that, we removed the samples from the mold and placed them in the water basin and they were kept in the laboratory environment at a temperature of 20 to 24 degrees Celsius for processing and testing at the desired ages.

Compressive and tensile strength tests were performed on concrete made at the ages of 5, 7, 28 and 90 days. 3 samples from each mixing plan were tested. The complete specifications of the plans are presented in Table 1. The compressive strength test was performed with 100x100x100 mm cubic samples according to the standard [24]. Cylindrical samples (150 x 300 mm) were also used to determine the tensile strength [25, 26].

3- Results

3-1- Slump

The results obtained from the fresh concrete test are shown in Table 7. The materials are at the workshop humidity level during mixing and are not in the SSD state, on the other hand, the water absorption of recycled materials is much higher. Therefore, in order to unify the consideration of water in mixing plans, the initial water of recycled mixing plans should be considered higher according to the consumption of recycled materials. As a result, at the beginning of mixing, designs containing recycled materials that have a higher initial water

silica in concrete samples causes an increase in slump. The reason for this could be that micro silica is basically a strong pozzolanic material that increases the adhesion of cement to aggregates and prevents the water absorption of aggregates and

content have higher efficiency. Therefore, according to this issue, smaller amounts of super-lubricant should be used for recycled designs in order to achieve almost the same efficiency of mixing designs and to prevent the concrete from dewatering and the separation of concrete particles [27].

In this research, the method presented in the ASTM-C143 standard [28] was used to determine the slump of fresh concrete.

According to the results, the replacement of recycled aggregates with natural aggregates has reduced the slump, which is due to the increase of voids in the recycled aggregates and, as a result, the reduction of the specific weight of recycled concrete [29].

Also, according to the results of Table 7, the use of polypropylene fibers has reduced the slump in samples containing natural and recycled aggregates and in equal conditions, the amount of slump in the samples containing polypropylene fibers and recycled aggregates has decreased to a greater extent than the samples containing natural aggregates and polypropylene fibers. In the conducted studies, it was determined that the reason for this could be the interference of the effect of fibers in creating voids and voids in recycled aggregates [30].

The addition of micro silica to the laboratory samples of this research has reduced the slump compared to the samples without micro silica. In general, micro

thus increases slump [31, 32]. It should be noted that in this research, different water-cement ratios in the mixing designs may have caused slump reduction in samples containing micro silica.

Table 7- Slump test results

Water to cement ratio	Design name	recycled concrete	Percentage of polypropylene fibers	super lubricant	silica fume	Slump(cm)
0.40	Pp0-rc0	0	0%	1%	40	9
	Pp1.5-rc0	0	1.5%	1%	40	7.5
	Pp0-rc100	100	0%	1%	40	7
	Pp1.5-rc100	100	1.5%	1%	40	6.5
0.55	Pp0-rc0	0	0%	0.8%	0	9.5
	Pp1.5-rc0	0	1.5%	0.8%	0	8.2
	Pp0-rc100	100	0%	0.8%	0	8
	Pp1.5-rc100	100	1.5%	0.8%	0	7

3-2- Compressive resistance

Compressive strength is one of the most important parameters for measuring the behavior of concrete. From the past until now, many researchers have improved the compressive strength of concrete by adding different additives and fibers. In this research, by combining polypropylene fibers in concrete containing natural and recycled aggregates, the compressive strength of concrete at the ages of 5, 7, 28 and 90 days has been investigated.

According to Table 8, by replacing recycled aggregates instead of natural aggregates, the compressive strength has decreased, the possible reason for this is that, firstly, waste concrete aggregates have high water absorption, secondly, recycled concrete aggregates have low density and thirdly, old mortar (mortar on recycled concrete aggregate) attached to recycled concrete aggregate has a weaker surface than the surface of natural aggregate. It should be noted that most of the studies conducted in the field of concrete with recycled concrete aggregate have a consensus opinion on the reduction of compressive strength [33-35]. Also, by using 1.5% of polypropylene fibers, the compressive strength has increased

somewhat. As it is clear from the results, the highest amount of compressive strength was obtained in the sample containing natural aggregates and polypropylene fibers, and the lowest amount of compressive strength was obtained in the samples without fibers and containing recycled aggregates.

Also, the results of the compressive strength in this research show that with the passage of time, the compressive strength of all the examined samples is increasing and the maximum strength of the samples was achieved in 90 days. Also, the highest rate of growth of compressive strength has taken place from 28 to 90 days. Diagrams 1 and 2 respectively show the compressive strength of the samples investigated in this research in two water-to-cement ratios (0.4 and 0.55). Also, micro silica pozzolanic material has been used in concrete samples made with a water-cement ratio of 0.4. As it is clear from the results, by adding micro silica to concrete samples, due to the strong pozzolanic property of micro silica, which has increased the adhesion of cement to aggregates, the compressive strength has increased [36].

Table 8- Compressive strength of fiber concrete samples containing natural and recycled aggregates

Water to cement ratio	Design name	Percentage of polypropylene fibers	recycled concrete	5 days (Mpa)	7 days (Mpa)	28 days (Mpa)	90 days (Mpa)
0.40	Pp0-rc0	0%	0	15.320	19.874	28.324	44.358
	Pp1.5-rc0	1.5%	0	17.514	21.247	30.145	46.214
	Pp0-rc100	0%	100	10.245	13.247	24.178	43.751
	Pp1.5-rc100	1.5%	100	13.547	14.796	25.386	44.971
0.55	Pp0-rc0	0%	0	13.850	18.357	27.014	43.744
	Pp1.5-rc0	1.5%	0	15.347	20.001	29.746	44.974
	Pp0-rc100	0%	100	9.745	11.389	22.159	42.775
	Pp1.5-rc100	1.5%	100	12.478	13.763	23.1	43.952

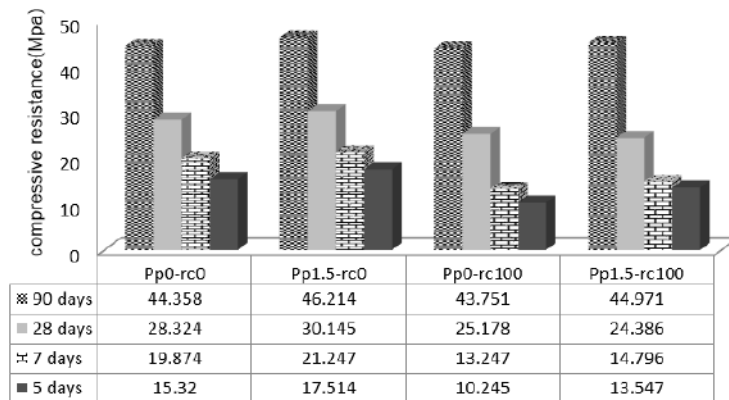


Chart 1- Compressive strength of concrete samples with 0.4 water-cement ratio and containing micro silica

The results of the tests show that the compressive strength only in the mixture of 1.5% fibers in all water-cement ratios, compared to the control sample, has resistance growth in all periods. But in

other mixtures, compared to the control sample, the amount of compressive strength has decreased, and with the passage of time and increasing age of the samples, the difference has decreased. This issue can be explained according to the activity of pozzolan used in this research.

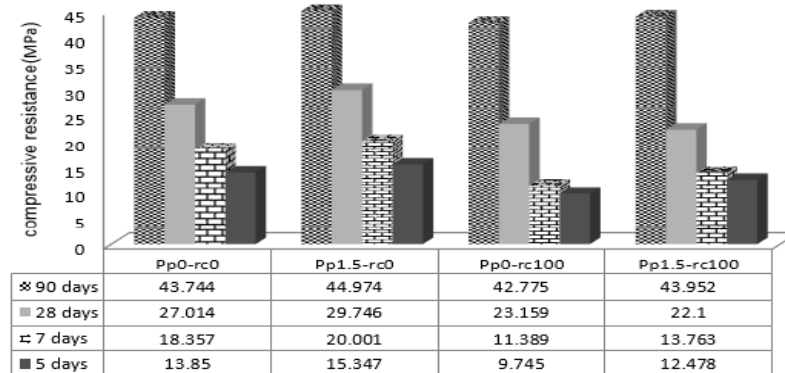


Chart 2- Compressive strength of concrete samples with a water-cement ratio of 0.55 and without micro silica

The strength loss factor in the mixtures compared to the control sample can be attributed to the excessive use of recycled concrete compared to the optimal amount. Of course, declaring a definite opinion is subject to more research and a more detailed examination of the microstructure of concrete.

3-3- Tensile strength

This test, which is also known as the Brazilian test, was carried out using standard cylindrical samples with a height of 30 cm and a diameter of 15 cm for 8 mixing designs at the ages of 5, 7, 28 and 90 days by dividing the concrete samples into two halves. Table 9 and graphs 3 and 4 show the tensile test results. As it is clear from the results, by replacing recycled aggregates instead of natural aggregates, the tensile strength of concrete has decreased, and the possible reason for this is that, firstly, waste concrete aggregates have lower resistance than natural aggregates, and also the presence of voids in recycled aggregates. It is another factor that can reduce the tensile strength in concrete samples made from these aggregates. It should be noted that most of the studies conducted in the field of concrete with recycled concrete aggregate have a consensus opinion on the reduction of tensile strength [33-35]. Also, the results show that by using 1.5% of polypropylene fibers, the tensile strength has increased to some extent. As it is clear from the results, the highest amount of tensile

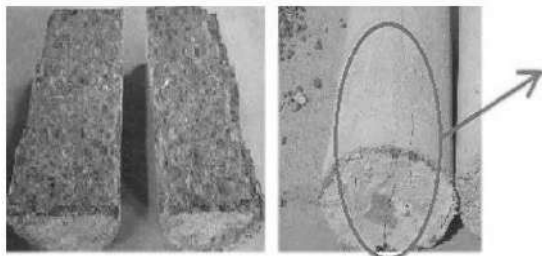
strength was obtained in the sample containing natural aggregates and polypropylene fibers, and the lowest amount of compressive strength was obtained in the samples without fibers and containing recycled aggregates.

Samples of concrete with fiber and without fiber after tensile strength test are shown in Figure 3. As it is clear from this figure, in concrete without fibers, after the test, the sample is completely separated and broken. But in fiber concrete, after testing on concrete samples, only small cracks can be seen and the concrete has maintained its cohesion and does not break apart. This article shows that fiber concrete does not crumble and break when broken and fibers play an important role in controlling concrete cracking. In fact, the fibers prevent their development and expansion by bridging the cracks. Therefore, the addition of fibers improves the brittle behavior of concrete.

Also, the results of tensile strength in this research show that with the passage of time, the amount of tensile strength is increasing in all the examined samples, and the maximum strength of the samples was achieved in 90 days. Also, the highest growth rate of tensile strength was observed from 28 to 90 days. Graphs 3 and 4 respectively show the tensile strength of the samples investigated in this research in two water-to-cement ratios (0.4 and 0.55). Also, micro silica pozzolanic material has been used in

Table 9- Tensile strength of fiber concrete samples containing natural and recycled aggregates

Water to cement ratio	Design name	Percentage of polypropylene fibers	recycled concrete	5 days (Mpa)	7 days (Mpa)	28 days (Mpa)	90 days (Mpa)
0.40	Pp0-rc0	0%	0	1.40	1.70	2.53	3.43
	Pp1.5-rc0	1.5%	0	2	2.11	2.88	3.64
	Pp0-rc100	0%	100	1.41	1.59	2.01	2.77
	Pp1.5-rc100	1.5%	100	1.54	1.73	2.28	2.89
0.55	Pp0-rc0	0%	0	1.33	1.60	2.5	3.35
	Pp1.5-rc0	1.5%	0	1.88	2	2.7	3.54
	Pp0-rc100	0%	100	1.10	1.41	2	2.69
	Pp1.5-rc100	1.5%	100	1.30	1.67	2.14	2.79



Maintaining the cohesion of concrete and controlling cracking by means of fibers

Figure 3- Comparison of recycled concrete with fibers (right side) and without fibers (left side) in terms of cracking and failure

concrete samples made with a water-cement ratio of 0.4. As it is clear from the results, by adding micro silica to concrete samples, the tensile strength has increased due to the strong pozzolanic property of micro silica which has increased the adhesion of cement to aggregates [36].

4 - Conclusion

The main goal of this research is investigating the use of recycled aggregates obtained from the destruction of concrete in the construction of new concrete has been for the protection of natural resources and sustainable development, Therefore, in this regard, in this research, we investigated and compared the mechanical properties of concrete containing natural and recycled concrete aggregates

and polypropylene fibers along with micro silica in two water-to-cement ratios of 0.4 and 0.55. According to the current investigation regarding the use of recycled aggregates and polypropylene fibers and micro silica, the following results have been obtained:

- Although the efficiency of concrete decreases due to higher water absorption by recycled aggregates and the use of polypropylene fibers, can be compensated by using materials such as super-lubricants. Considering that polypropylene fibers also improve the behavior of structural concrete.

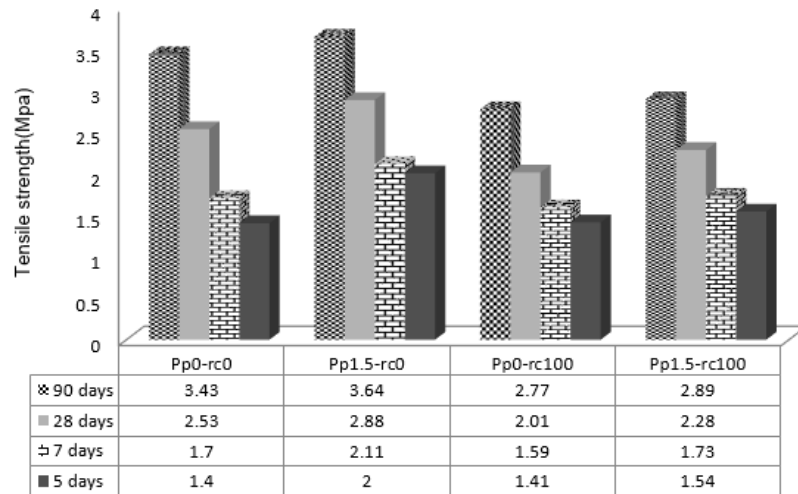


Diagram 3- Tensile strength of concrete samples with 0.4 water-cement ratio and containing micro silica

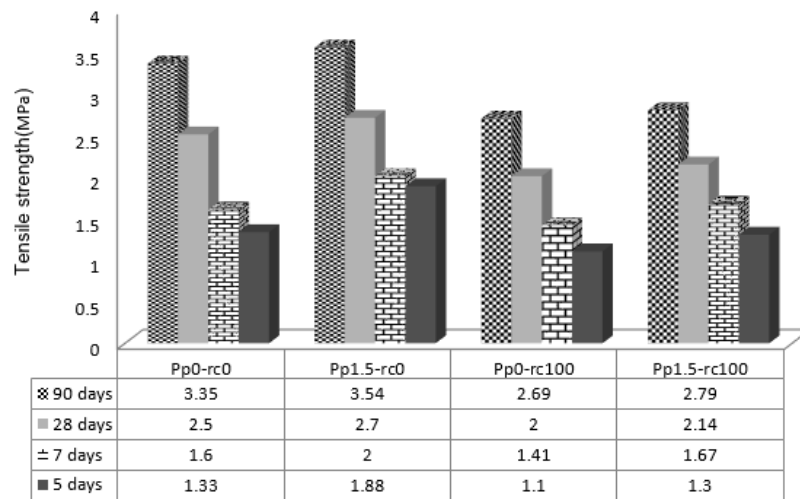


Diagram 4- Tensile strength of concrete samples with a water-cement ratio of 0.55 and without micro silica

- If recycled aggregates are used, the compressive and tensile strength of the samples decreases, but the addition of fibers and micro silica improved the tensile and compressive strength performance to some extent.

- With the passage of time in all the mixing plans, the compressive and tensile strength of the samples increased, and the greatest increase in strength was from the age of 28 to 90 days.

- Observations related to the failure of concrete tensile samples showed that the presence of fibers in concrete delays the initial cracks and prevents the crushing of concrete, which is a brittle material by nature. In fact, the fibers in concrete bridge the cracks and prevent the crack from spreading.

- Considering the results of this research in the direction of protecting natural resources and sustainable development, fiber recycled concrete can be used in applications where tensile and compressive strength and concrete cracking control are important. Among these cases, we can mention the paving of roads, runways, industrial floors, construction of prefabricated building parts including canopy panels, concrete of curved surfaces such as tunnels.

Refrence

- [1] Ann K Y, Moon H, Kim Y, Ryou J. Durability of recycled aggregate concrete using pozzolanic materials. *Waste Management*, 28(6): 993-999, 2008.
- [2] Awoyera P, Okoro U. Filler-ability of highly active metakaolin for improving morphology and strength characteristics of recycled aggregate concrete. *Silicon*, 11(4): 1971-1978, 2019.
- [3] Hansen T C. Recycling of demolished concrete and masonry. CRC Press, 1992.
- [4] Liu J, Gong E, Wang D, Lai X, Zhu J. Attitudes and behaviour towards construction waste minimisation: a comparative analysis between China and the USA. *Environmental Science and Pollution Research*, 26(14): 13681-13690, 2019.
- [5] Ostyakova A, Mazurin D. Management of the waste of construction and demolition, in: IOP Conference Series. Materials Science and Engineering, IOP Publishing, pp. 012103, 2021.
- [6] Malbora V, Neville M. Symposium on concrete technology in use of demolition waste in concrete. By Wain Wright, PJ 26: 179- 197, 1995.
- [7] Durmus G, Sims O, ek M. The effects of coarse recycled concrete aggregates on concrete properties, *J. Fac. Eng. Archit. Gazi Univ.* 24: 183–189, 2009.
- [8] Xiao J, Li W, Fan Y, Huang X. An overview of study on recycled aggregate concrete in China 1996–2011, *Constr. Build. Mater.* 31: 364–383, 2012.
- [9] Limbachiya M.C Leelawat T, Dhir R.K. Use of recycled concrete aggregate in high-strength concrete. *Mater. Struct.* 33: 574–580, 2000.
- [10] Eguchi K, Teranishi K, Nakagome A, Kishimoto H, Shinozaki K, Narikawa M. Application of recycled coarse aggregate by mixture to concrete construction, *Constr. Build. Mater.* 21: 1542–1551, 2007.
- [11] Thomas C, Setien J, Polanco J.A, Alaejos P, De Juan M.S. Durability of recycled aggregate concrete. *Constr. Build. Mater.* 40: 1054–1065, 2013.
- [12] Sheen Y.N, Wang H.Y, Juang Y.P, Le D.H. Assessment on the engineering properties of ready-mixed concrete using recycled aggregates. *Constr. Build. Mater.* 45: 298–305, 2013.
- [13] Evangelista L, De Brito J. Durability performance of concrete made with fine recycled concrete aggregates. *Cement and Concrete composites*, 32: 9-14, 2010.
- [14] Wai H K, Mahyuddin R, Kenn J K, Mohd Z S. Influence of the amount of recycled coarse aggregate in concrete design and durability properties. *Construction and building materials*, 26: 565-573, 2012.
- [15] Shi-Cong K, Chi-Sun P, Miren E. Influence of recycled aggregates on long term mechanical

properties and pore size distribution of concrete. cement and concrete composites. 33: 286-291, 2011.

[16] Carneiro J.A, Lima P.R.L, Leite M.B Toledo Filho R.D. Compressive stress–strain behavior of steel fiber reinforced-recycled aggregate concrete. Cement and concrete composites, 46: 65-72, 2014.

[17] Akça K.R, Çakır Ö, İpek M. Properties of polypropylene fiber reinforced concrete using recycled aggregates. Construction and Building Materials, 98: 620-630, 2015.

[18] Jalilifar H, Sajedi F, Kazemi S. Retracted: Investigation on the Mechanical Properties of Fiber Reinforced Recycled Concrete. Civil Engineering Journal, 2(1): 13-22, 2016.

[19] Malisch WR. Polypropylene Fibers in Concrete, What do the test tell us? Concrete Construction. 31(4): 363-368, 1996.

[20] Alves M, Cremonini R, Dal Molin D. A comparison of mix proportioning methods for high-strength concrete. Cement and Concrete Composites, 26(6): 613-621, 2004.

[21] Jokar F, Khorram M, Karimi G, Hataf N. Experimental investigation of mechanical properties of crumbed rubber concrete containing natural zeolite. Construction and Building Materials, 208: 651-658, 2019.

[22] Kapoor K, Singh S, Singh B. Durability of self-compacting concrete made with Recycled Concrete Aggregates and mineral admixtures. Construction and Building Materials, 128: 67-76, 2016.

[23] ASTM C131. Standard Test Method for Resistance to Degradation of Small-Size Coarse Aggregate by Abrasion and Impact in the Los Angeles Machine.

[24] EN 12390-3, Testing Hardened Concrete – Part 3: Compressive Strength of Test Specimens, 2009

[25] EN 12390-6, Testing Hardened Concrete – Part 6: Tensile Splitting Strength of Test Specimens, 2009.

[26] ASTM C143/C143M - 15a Standard Test Method for Slump of Hydraulic Cement Concrete.

[27] Ferreira L, Brito J, Barra M. Influence of pre-saturation of recycled coarse concrete aggregates on structural concrete's mechanical and durability properties. Magazine of Concrete Research. 2017.

[28] Conshohocken P. ASTM International, Atanasova, B., Langlois, D., Nicklaus, S., Chabanet, C. et Etiévant, P, 2004.

[29] Azúa G, González M, Arroyo P, Kurama Y. Recycled coarse aggregates from precast plant and



The role of advanced crisis management in providing relief during an earthquake using the location of vulnerable areas based on the risk matrix (case study: Lahijan city)

Sahebeh Kheirkhah Ghorbani ^{a*}

^aDepartment of Civil Engineering, Chalous Branch, Islamic Azad University, Chalous, Iran

Journals-Researchers use only: Received date: 2022.10.20; revised date: 2022.11.15; accepted date: 2022.11.20

Abstract

In general, crisis management means purposefully pushing the progress of affairs to a controllable routine and expecting things to return to the pre-crisis conditions as soon as possible. In short, crisis management is all actions related to prevention and risk management, organization and management of resources needed in response to crisis. Crisis management is an applied science that, through systematic observation of crises and their analysis, seeks to find tools that can be used to prevent the occurrence of crises or, in case of occurrence, in terms of reducing the effects of the crisis, necessary preparation and rapid relief, and took action to improve the situation. The main purpose of this research is modern crisis management in the probability of an earthquake based on risk matrix by locating vulnerable areas in Lahijan city using AHP, TOPSIS and SWOT analysis. © 2017 Journals-Researchers. All rights reserved. (DOI:<https://doi.org/10.52547/JCER.4.4.33>)

"Keywords: Crisis management, Feasibility study, AHP hierarchical analysis."

1. Introduction

Today's life continues while the shadowing of uncertainty on all matters has completely transformed the decision-making process for various reasons. Technical changes along with other environmental changes of organizations have caused the emergence of new scientific ideas in the field of risk and its

management. In management decisions, there is no topic more necessary and important than risk assessment and crisis management. Engineers, contractors and designers in the implementation of construction projects usually try to create a suitable combination between risk and return, so that they can minimize the risk by planning and managing it. In fact, it is not about finding an acceptable investment solution, but rather determining a suitable situation for crisis management. In fact, risk is an integral part

* Corresponding author. Tel.: +98-935-289-1712; e-mail: hadiskheirkhah87@gmail.com.

of people's and organizations' lives, and all decision-making situations face a variety of risks. Taking risk is not bad in itself, the important thing is not to be exposed to risk for no reason. Human life is intertwined with the acceptance of risk in such a way that perhaps the absolute lack of risk-taking causes human life to be placed in a lower order than the current level. Also, the traditional attitude towards advanced crisis management was to believe that crisis management means putting out the fire; This means that crisis managers sit waiting for things to break down and after the destruction occurs, they try to limit the damage caused by the breakdowns. But recently, the attitude towards this word has changed. Based on the latter meaning, a set of practical plans and plans should always be prepared to face possible future developments within organizations, and managers should think about possible future events and prepare to face unforeseen events; Therefore, crisis management emphasizes the necessity of regular forecasting and getting ready to face those internal and external issues that seriously threaten the reputation, profitability, or life of the organization. It should be noted that crisis management is different from public relations management. The public relations manager tries to make the organization look good while the crisis manager tries to keep the organization in a good position in difficult situations. Crisis management as a scientific discipline is generally placed in the field of strategic management and is specifically related to strategic control topics. Urban communities need to maintain security, psychological comfort, lack of disturbance and structural disorder, and in terms of the psychology of urban environments, they demand optimal organization in order to achieve the goals and strategies of the city, against any danger. Also, evaluating the course of evolution and how the management practices of the city have changed during different historical periods can determine the relativity of the city's approach in understanding the events that may occur in the future as accurately as possible.

2. Method of Study

This research is one of the quantitative researches and in terms of its purpose, it is one of the exploratory researches, because it seeks the role of advanced crisis management in providing relief during an earthquake by using the location of vulnerable areas based on the risk matrix (case study: Lahijan city). Also, due to the fact that the information of the investigated community was collected using interviews, this research is a survey research and in terms of the type of study, it is a case study.

The method of this research is analytical and descriptive and the comparative method will be used to summarize the findings and determine the vulnerable points. The tools of this research will include documentation and library resources and the preparation of a researcher-made questionnaire. This research will first examine the degree of vulnerability of the studied area during an earthquake, and by collecting the questionnaire and determining the criteria affecting the degree of damage using the series method. AHP levels are taken into consideration and location of vulnerable points using SWOT analysis technique will determine weaknesses and strengths, opportunities and threats and strategies, policies or measures will be presented to reduce its vulnerability and advance aid delivery.

3. Analysis Proseccos

In this research, the weighting model of the multi-criteria method has been used, in which the factors that are effective in determining the location are determined first.

In the next step, these indicators are quantified. In the third stage, points are given to these factors based on their quantity. In the fourth step, in order to obtain the total score of each area, instead of adding up the scores of each factor, one can assign a weight to each of them, and then calculate the weighted sum of the total score.

In other words, after determining the effective factors:

- Each factor is assigned a weight.

- The degree of location selection is known for each factor.

- The weight distribution of the factors is calculated among the resulting accumulation.

- Weighted density is obtained for each area.

- The place or places that have the maximum weight are chosen as the right place.

Also, based on the primary and secondary data, first the spatial data digitized from the existing maps in the storage and maintenance system, then the

required non-spatial (descriptive) data is attributed to each condition. In this way, by using the stored spatial database and non-spatial database, the geographic information system is produced and the possibility of retrieving, deleting and adding, classifying and analyzing data using factors that are effective in choosing a place is provided. becomes The result of the analysis is the production of a map in which suitable areas are specified.

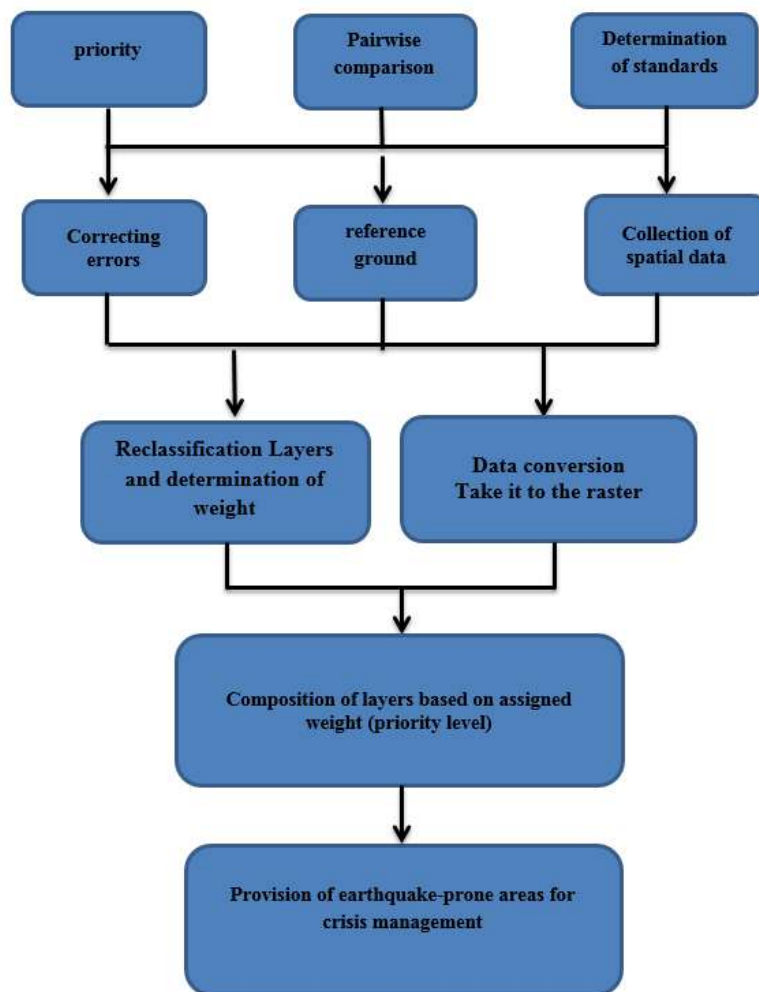


Figure-1- Schematic design of positioning model

4. Data Analysis:

In the multi-factor evaluation, different physical factors and economic and social conditions of the region are used to determine the intended use. Land suitability for a specific type of use can be determined by evaluating multi-factor techniques. Suitability of use for a specific use depends on the characteristics of that place and its topological relationship with its environmental factors. The most important characteristic of the multi-factor evaluation method is the method of combining and analyzing information, considering that in the multi-factor evaluation, different parameters are analyzed, so this increases the complexity of the evaluation process.

Based on this, geographic information is increasingly used by specialists in the identification of terrestrial phenomena and the analysis of the obtained information.

The geographic information system can be considered as that part of database management that provides both technology and software for obtaining, storing and retrieving, processing and displaying spatial information. The geographic information system widely displays available information on two-dimensional maps and focuses on equipment and facilities to integrate and analyze information.

The geographic information system provides tools to support spatial information to evaluate multiple factors in order to reach a logical and justifiable decision.

The use of multi-agent techniques in the geographic information system is based on a logical method that provides the necessary tools for analysis and planning.

Using the multi-factor evaluation method requires operations, the most important of which are:

- 1- Identification of effective factors in evaluation
- 2- Standardizing the values in the maps of the evaluated factors
- 3- Determining the coefficients of effective factors in evaluation
- 4- Method of analysis of effective factors in evaluation.

Standardizing data means equalizing the range of data change between zero and one [1 and 0].

Effective factors in evaluation usually have a different nature from each other and their measurement criteria are different from each other.

In order to effectively use all the factors in the analysis and establish a relationship between them, the existing values are normalized to each of the effective factors in the evaluation under a special rule, which is called data standardization.

For this purpose, methods similar to those used in satellite data processing to increase the contrast between classes and improve the quality of information are used. AHP, TOPSIS and SWOT methods were used in this research.

5. Hierarchical AHP analysis

Hierarchical analysis process is one of the most comprehensive systems designed for decision making with multiple criteria. At the same time, this technique provides the possibility of formulating the problem hierarchically, creating a combination of different quantitative and qualitative criteria [1].

AHP is a mathematical method for analyzing complex problems with multiple criteria. This method was first presented by Thomas L. Saaty. This process begins with the identification and prioritization of decision making elements. These elements include goals, criteria, characteristics and possible options that are used in prioritization [2].

In this method, after creating a tree or hierarchical structure of decision-making elements (objectives, criteria and options), a two-by-two comparison of each level of elements is made, thus determining the weight of each element in a cluster or level and in order to ensure the stability of the determined weights to achieve the desired goal, calculate their compatibility rate.

Hierarchical analysis is a process that can easily reflect the change of environmental factors and obtain appropriate results. This process helps the members to identify the variables that are subject to drastic changes and also facilitates the calculation of these changes [1].

Analysis is very compatible with the way of thinking and mental processes of humans and can

Table-1- 9 hourly quantitative scale for binary comparison of options

explain	Definition	Score (severity of importance)
In achieving the goal, two criteria are equally important	Equal importance	1
.Experience shows that i is slightly more important than j to achieve the goal	A little more important	3
.To achieve the goal, i is more important than j	more important	5
.To achieve the goal, i is much more important than j	Much more important	7
.The much greater importance of i than j has been definitely proven	Absolute importance	9
When there is an intermediate state		

Table-2- The matrix of the main research criteria

Socio-economic conditions	Features of the shape of the earth	Weather and climate conditions	Criteria
1/5	3	1	Weather and climate conditions
1/5	1		Features of the shape of the earth
1			Socio-economic conditions

take advantage of people's verbal opinions and judgments during decision-making and make decisions individually and in groups [3]. In the hierarchical analysis model as a decision-making model, one of the main sources of analysis data is the opinion of the decision-makers themselves [4].

Up to this stage, the importance coefficients of criteria and sub-criteria and options have been determined in relation to the purpose of the study. At this stage, the "final score" of each sub-criteria will be determined by combining the importance coefficients. For this purpose, the hourly "Principle of Hierarchical Composition" will be used, which leads to a "Preference Vector" considering all judgments at all hierarchical levels. According to the analysis done by Expert Choice software, the relative weight of each risk is calculated according to the probability of an earthquake.

The "final score" of each option is determined by combining the importance coefficients of the criteria in relation to the purpose of the study, as well as the importance coefficients (score) of the options in relation to each of the sub-criteria. The method of determining the final score of options is based on the hourly "principle of hierarchical composition" and using importance coefficients that lead to a "priority vector" considering all judgments at all hierarchical levels:

$$\sum_{k=1}^n \sum_{i=1}^m W_k W_i (g_{ij}) = \text{final score (priority)}$$

of option j

where in:

W_k = importance coefficient of criterion k

W_i = importance coefficient under criterion i

g_{ij} = score of option j in relation to sub-criterion i

Offensive strategies (S-O): are strategies that seek to take advantage of opportunities and are well coordinated with the organization's capabilities.

Protection strategy (W-O): overcoming weaknesses in order to take advantage of opportunities.

Competitive strategy (S-T): Identifying methods that the organization can use to reduce its vulnerability from threats.

Defensive strategy (W-T): a completely defensive strategy that prevents the organization from being harmed due to its weaknesses from threats from the external environment.

6. QSPM matrix analysis

In this study, also from the quantitative strategic planning approach (Quantitative Strategic Planning Matrix). It was used to prioritize strategies. The QSPM quantitative strategic planning matrix is also an analytical method that provides managers with the

possibility of evaluating alternative strategies based on internal and external influencing factors.



Figure-3- The strategic situation of earthquake feasibility in Lahijan city and crisis management in this city

With this method, various strategies were determined objectively, which are among the best strategies. Management strategies in this research were obtained by using different tools and in three general stages including information entry, their comparison and decision making stage (Figure 3).

In the input phase, the main information needed for the formulation of strategies was determined. After that, internal factors evaluation matrix (IFE) and external factors evaluation matrix (EFE) were implemented.

The information obtained from this stage provides a basis for comparison (third stage) and by considering them, different strategy options can be identified and evaluated in order to choose the best strategies. By determining the cumulative effects of each of the internal and external factors, the relative attractiveness of each of the strategies can be determined.

In order to provide a quantitative strategic evaluation matrix, six steps were followed as follows:

1- Major external opportunities and threats and major internal strengths and weaknesses were reflected in the strategic planning matrix. This information is obtained directly from the evaluation matrix of internal and external factors. At least 13 very important external factors and 12 very important internal factors were paid attention to in setting up the QSPM matrix.

2- A weight or coefficient was given to each of the internal and external factors. These coefficients are

just like the coefficients of the evaluation matrix of internal and external factors;

3- The compiled strategies were written in the top row of the matrix;

4- Then the attractiveness scores were determined. The attractiveness score shows the power and ability of the strategy in dealing with internal and external factors (taking advantage of strengths and opportunities and eliminating weaknesses and avoiding threats), which was entered as follows: 1 = no attractiveness, 2 = up to somewhat attractive, 3 = reasonably attractive and

4 = very attractive;

5- The attractiveness score of each strategy is calculated from the sum of the product of the importance coefficients in the attractiveness scores. The sum of the attractiveness scores indicates the relative attractiveness of each strategy, which is obtained only by considering the effect of the relevant internal and external factors.

The higher the sum of attractiveness scores, the more priority the discussed strategy will have.

High scores indicate a higher attractiveness of the strategy

7. Discussion:

Cities have a physical space, each of these bodies contains an activity, and all of them make the city space and give it an identity. Cities are defined by human concentration centers, human activities and buildings.

The urban space contains infrastructure facilities and equipment with all kinds of uses, including residential, office, service, health, etc. The above categories will lead to a dependent population, which is greatly affected by the occurrence of natural disasters and causes unrest in the life system and many human and financial losses in the cities.

The occurrence of unexpected events in the history of human life has always had a limiting and effective role and has left many effects; Therefore, how to deal with these crises is one of the constant anxieties of human societies. The methods of dealing with these crises can intensify and mitigate its negative effects. The feasibility planning process of seismic areas is very important; If this process is not

logical and calculated, the probability of the produced programs being valuable will be low.

Preparation of crisis management plans is considered a basic step in crisis containment, but these plans will have the necessary efficiency when they are regular and up-to-date, as well as their effectiveness, especially those parts that are related to the reaction and response phase in a crisis. are related, there is sufficient assurance.

The geography of Gilan province with favorable natural and artificial opportunities is prone to improve crisis management and select suitable areas for settlement.

But these opportunities require a will to overcome challenges and bring these opportunities to their destination in an action plan. Also, scientific manipulation and intervention by preserving the originality of nature can lead to consolidation of crisis management foundations in the province, especially in Lahijan city.

Feasibility or feasibility studies is the assessment and analysis of the potential of a proposed project and is based on research and studies that support the decision-making process.

Feasibility discusses whether things are possible. Feasibility studies are carried out after the stage of creation of the plan and definition of its general framework in terms of the general characteristics of the product, production capacity and investment amount. These studies can be included in different levels of project details according to the needs and requests of the employer.

In fact, the feasibility study in this study was conducted on the earthquake-prone areas of Lahijan city in order to prevent casualties and financial and life losses in sensitive areas.

8. Conclusion:

Proper location is always the first and most important step in the crisis management process. In this regard, one should try to choose suitable areas based on the limitations and capabilities required by the plan. It should be noted that the studies required for location are very extensive and by using satellite images and geographic information system, an

important part of these studies can be done without physical presence in the region. The land and the shape of the land is the stage on which structures play a role. Lowlands and elevations, drainage patterns, geology and soil are some of the factors related to the shape of the land.

Designers, aviators, and astronauts see the same mountains, valleys, plateaus, and lowlands, but relief workers and crisis management consultants, who deal with details rather than pictures, have very different perspectives; Therefore, in the operation that takes place in the tactical category, natural complications should be well known. In the area that is chosen for crisis management and loss prevention, issues such as: the type of rocks, the resistance of the rocks, the slope of the slope, the location of the area in terms of natural hazards such as; Earthquakes, floods, falls, landslides, the effect of wind on the ground, heights overlooking the area, erosive activities of precipitation and temperature, the amount of soil moisture, etc. must be considered.

It is obvious that any kind of management can be done if, at the time of Talah, one acts to identify and examine the shapes and complications of the ground surface and study them accurately, and the battlefield recognizes the position of oneself and the enemy by knowing the shapes of the ground. and took the necessary measures.

In order to identify earthquake-prone places in Lahijan city, variables such as: temperature, freezing days, drought, distance from the fault, slope direction, degree of slope, distance from water sources, distance from power plants, access to suitable roads, distance from Airport, distance from railways, distance from urban and rural areas, access to healthcare services, distance from commercial and industrial complexes and gas fields, distance from pipelines, compliance with distance from air corridors, distance from ports were investigated. The results showed:

1- According to AHP analysis, the criterion of socio-economic conditions with a weight of 0.53 was the most important criterion selected according to experts.

2- According to the results of the TOPSIS analysis, the distance from urban and rural areas (0.930) is the most related to the sub-criterion.

3- According to the analysis, region 2 has been selected as the most seismic place for crisis prevention and management with 0.684.

4- According to the SWOT analysis, the total of internal factors is greater than zero and equal to 0.423 and this indicates that the strengths are more than the weaknesses.

5- According to the SWOT analysis, the sum of external factors that is greater than zero and equal to 0.254, it can be said; Opportunities are more than threats.

6- In the selected location, 9 internal strengths against 4 internal weaknesses and 8 opportunities against 4 threats have been identified and investigated. In this way, a total of 17 strengths and opportunities were identified as advantages and 8 weaknesses and threats were identified as limitations and bottlenecks in choosing a suitable location for crisis management in Lahijan city.

7- According to the score obtained from the final sum of the matrix of internal factors, it is concluded that in the feasibility of earthquake-prone areas in Lahijan city with the current situation, the strengths for crisis management are more than its weaknesses.

8- Based on the obtained values and according to the matrix, out of the four possible strategies, the optimal strategy for crisis management in Lahijan city, SO or offensive strategies, was proposed and used.

9- The results of the Quantitative Strategic Planning Matrix (QSPM) show that among the prepared strategies, the highest attractiveness is related to the strategy of logistic support and flexibility, and the lowest attractiveness is related to the strategy of increasing utility costs (water, electricity, gas).

Geography and Urban Planning, University of Tehran. Iran, 2017.

- [4] H. Ziari, P. Karii, Proc. 4th National Civil Engineerin. Conf., Tehran, 5-6 May., 2008.

References

- [1] S. H. Ghodsyour, Analytic Hierachy Process, Amirkabir university of technology , Tehran, Iran, 2020 (In Persian).
- [2] E. Zebardast, Application of Analytic Hierachy Process in urban and regional planning, vol. 10, Honar-Ha-Ye-Ziba, IRAN, 2002.
- [3] Amini Varki, Saeed, Shamsai Zafarkandi, Fath Elah, Ghanbari Nasab, Ali, Identifying the ruling views on the vulnerability of cities to environmental hazards and extracting the influential components in it using Q method, Journal of



Analytical and Experimental Study of Load-bearing columns Made of Lightweight Concrete

Ghasem Azizi Daronkolaie ^{a*}, Mohsen Abzan ^b

^aEngineering faculty, Chalous Branch, Islamic Azad University, Chalous, 46615-397, Iran

^bEngineering faculty, Behshahr, Iran

Abstract

In recent years, studies have been started for the use of light-grained concrete in conventional reinforced concrete structures, it is expected that the use of light-grained concrete without having a negative effect on the use of the structure will reduce the costs in construction and reduce the structural mass. As a result, the earthquake load will be reduced. In this research, concrete with an approximate compressive strength of 18.24 megapascals and an approximate specific weight of 1800 kg/m³ was obtained by using Lika grain style. In order to evaluate the structural behavior of lightweight concrete, 5 concrete columns were built in the laboratory and were subjected to axial load and the results related to these columns were presented, and then a suitable model for these columns was presented by Abaqus finite element software and analytical studies. It was done on the relevant results, which are in good agreement with the laboratory results. The agreement of the results obtained from the modeling with the laboratory results is a proof of the accuracy of the built model. © 2017 Journals-Researchers. All rights reserved. (DOI: <https://doi.org/10.52547/JCER.4.4.41>)

Keywords: lightweight concrete column, finite element analysis, laboratory study, compressive behavior of columns, Abaqus.

1. Introduction

In recent years, the use of lightweight concrete in its various forms, such as lightweight concrete, concrete without fine grains or concrete with air bubbles, has become very common, and due to its

unique advantages such as low specific weight and good thermal insulation, in many cases it has replaced ordinary concrete. In this connection, it is possible to mention the implementation of some high-rise buildings and large bridges with this material, such as 15 large span bridges made of lightweight Leica concrete in the Netherlands,

* Corresponding author. Tel.: +98-911-114-0347; e-mail: ghasem.azizi.d@gmail.com

Wellington Stadium in New Zealand, and a 73-story commercial tower in Los Angeles.

The low strength of lightweight concrete has been an important factor in limiting the scope of application of this type of concrete and taking advantage of its advantages. Lightweight concrete that has sufficient strength and its other physical properties are also improved due to weight reduction will bring about a huge change in the application of this concrete.

Aggregates with less weight are generally considered as light grains [1]. For comparison, most common aggregates such as sand and gravel weigh up to 1680. The light grains have a low apparent specific gravity due to high porosity. The classification of seed styles is based on their sources, production methods and final use.

The main materials in the style of natural grains are diatomite, pumice, scoria (pumice stone), ash and volcanic tuff, all of which except diatomite are of volcanic origin. Diatomite has a sedimentary origin. Considering that natural grain styles are found only in some places, therefore, due to the problems of access to resources and transportation issues, this type of material is not widely used and has limited applications. Pumice has been used more than other types of these materials [2].

Artificial seed styles are often known by their different trade names. But the best grouping is based on the raw materials used and the production method. Artificial aggregates are produced in four ways. In the first method, artificial aggregates are obtained by heating and expanding clay, diatomaceous earth, perlite, vermiculite and opsidin. In the second method, molten slag from slag furnaces is obtained. By spraying controlled amounts of water, it expands with the help of a water jet. In the third method, industrial welds obtained from coal furnace ash are used. In the fourth method, light grains are produced from organic compounds such as expanded polystyrene. In Iran, only the first method is used to produce expanded clay and expanded perlite.

The properties of different grain styles are widely variable. For example, the strength of concrete made with expanded clay (Leica) and expanded shale is relatively high and comparable to normal concrete. Of course, the amount of cement used in light concrete is more than its amount in ordinary concrete.

Pumice, scoria and some expanded welds produce concrete with medium strength. Perlite, vermiculite and diatomite produce concrete with very low resistance, but the insulating properties of low resistance concrete are better than high and medium strength concrete. The insulation value of high resistance style concrete is almost 4 times that of ordinary concrete. In practice, there is a complete spectrum of grain styles with a weight of 80 to 900.

Very porous aggregates are generally weak and are more suitable for making non-structural insulating concrete. It is the grain style that has less porosity, if the structure of the porosity is in the form of small pores and with uniform distribution, then the grain style has strength and is therefore suitable for structural concrete.

There are three general methods of producing lightweight concrete. In the first method, light porous materials with low specific gravity are used instead of ordinary aggregates. The resulting concrete is called light grain concrete. The second method of producing light concrete is based on the creation of multiple pores inside the concrete or mortar. These pores should be clearly cleaned from very small pores with air bubbles. This type of concrete is known as "sponge concrete", "aerated concrete" or "gas concrete". The third method of producing light concrete is to remove small aggregates from the concrete mixture so that many pores are created between the particles and generally coarse aggregates with normal weight are used. This type of concrete is called "concrete without fine grains".

Despite the high cost of light grains and the additional initial cost of using light concrete, the total cost of a structure made with light concrete is less than normal concrete. The use of lightweight concrete in prefabs reduces its weight by half, which saves transportation costs. This savings well covers the additional costs of light grain materials. Sometimes, the dead load of a prefabricated piece is close to/or more than the crane used in the factory or workshop. By using light grains, due to weight reduction, the use of a special crane is not necessary and it is possible to make larger pieces than normal concrete. It also results in a reduction in crane movements. The economic advantages of light concrete can be divided into 2 categories:

One is the points due to less dead load, and the other points are points due to properties such as: more thermal insulation, resistance to fire, freezing, etc.

According to the studies conducted in recent years, to use light-grained concrete in conventional reinforced concrete structures, considering maintaining the durability and stability of the structure and reducing costs in construction, using light-grained concrete is a suitable solution, which in addition to reducing costs In construction, it reduces the structural mass and consequently reduces the earthquake load. Therefore, in this research, we evaluated the structural behavior of columns made of light-grained concrete, and then analytical studies were conducted on the results of these columns using Abaqus finite element software, and conclusions were drawn.

The second part of this research is an overview of the research done in the field of lightweight concrete. In the third part, the studies were described, which are in two phases, laboratory and modeling with Abaqus software. In the fourth part, the obtained results are analyzed and finally, the fifth part deals with general conclusions and suggestions for future studies.

2. Related works

Myatt et al [3] investigated the behavior of spiral structural columns made of lightweight concrete under central axial loading. In this experiment, Lika was used as lightweight coarse aggregate to produce lightweight concrete. A total of 11 columns were evaluated under short-term loading. The columns were made with a height of 900 mm and a diameter of 250 mm. The studied parameters include diameter and spiral reinforcement. The final strength of the columns is reduced, also the area of the longitudinal reinforcement does not affect the ductility of the column, in addition, the steel fibers in the spiral reinforcement of the columns leads to an increase in the final fineness of the column, although it has a small effect on the ductility.

Galeota et al. [4] investigated the ductility and resistance in the performance of structural columns made of light-grained concrete. that the arrangement

of transverse reinforcement, spacing of transverse reinforcement and the ratio of longitudinal reinforcement in the structural performance of columns made of light-grained concrete under uniform off-center loading were investigated, the experimental results show that the use of reinforcement arrangements The following transversal leads to significant improvement in structural performance.

Kan et al. [5], which evaluated the behavior and size effect of structural columns made of light-grained concrete and 3 other square columns made of ordinary concrete in different sizes, the test results showed that the columns Made of light-grained concrete, they have the same failure mode as the columns made of ordinary concrete. Also, under the same axial load, they show a larger displacement than the columns made of ordinary concrete. Measurement of the ultimate strength of the column. made of light-grained concrete with small and medium sizes were obtained close to the calculated values of the ACI nominal strength, which shows that the ACI equation is only suitable for the design of small and medium-sized columns.

Qonem et al. [6] conducted an experimental study on steel pipes filled with light-grained concrete, and these experiments were carried out on steel tubular columns with circular and rectangular sections filled with light-grained concrete and In this study, columns filled with light-grained concrete show local buckling, when the column reaches the breaking load, a global buckling takes place. However, the effect The negative local buckling does not significantly decrease the capacity with the bearing capacity of the column, but the columns filled with ordinary concrete show global buckling without any signs of local buckling before failure, also the sections with larger dimensions of the bearing capacity. It shows that according to these results, there is a good possibility of replacing normal concrete with light-grained concrete due to its low specific weight and thermal conductivity.

Moli and Khalafi [7] investigated the strength and axial capacity of steel columns filled with light-grained concrete, and this test was a set of 2 hollow rectangular steel sections with dimensions of 120x80 mm and 150x100 mm and different heights. These sections were filled with ordinary concrete and light-

grained concrete, natural pozzolan was used as lightweight aggregate in the second concrete, and in this test, the performance of steel samples filled with light-grained concrete compared to steel samples It was made of ordinary concrete. The test results showed that the breaking load is affected when the height of the samples increases from 100 mm to 200 mm, and also the presented lightweight concrete has a higher resistance than ordinary concrete.

3. Laboratory studies have been carried out

The main goal of this research is to achieve structural light concrete with lower specific weight and higher compressive strength. Based on this, in this experiment, 5 cubic samples of 10x10x10 cm were made and after 28 days of curing in water, their specific weight and compressive strength were determined.

3.1. Consumable materials

The cement used was Portland type 2 neka and potable water was used to make concrete. Consumable micro-silica is in the form of powder produced by Vand Chemical Company, and the specific surface area of its particles is 20. In this research, 10% of the weight of cement was replaced with micro-silica and the amount of cement was reduced by the same amount. PCE super plasticizer was also used. The amount of PCE is about 1.5-4% of cement materials. At the beginning, the sand used was passed through a sieve with a score of 4, therefore, sand with a size of 0-5 mm was used in the concrete. Its modulus of elasticity was equal to 2.6.

In table (3-4) the sand classification is presented. The granulation of used sand has an acceptable match with the permissible range of natural sand.

In this research, the size of 5-10 mm and discontinuous granulation was chosen. Natural sand has been used instead of 0-5 mm Leica grains. One-hour water absorption of Leica seeds is 11.3%. For granulation, 500 grams of Leica was selected. The tested fine grain does not have an acceptable compliance with the permitted range of fine grain sand with a maximum size of 12.7 mm. According to the granulation, the Leica used is coarse-grained.

The inner armature is ribbed and type AIII. The yield stress of rebar grade 10 is 4800 and the yield stress of rebar grade 8 is 4930.

After carrying out some preliminary mixing plans for preparing light concrete with suitable structural strength for the intended columns, the mixing plan of Table 1 has been used:

Table 1

Light concrete mixing plan for one cubic meter of concrete

micro-silica (kg)	475
Cement (kg)	47.5
Water (kg)	7
Super lubricant (kg)	199.5
Leica (kg)	803
Sand (kg)	268
Leica size (mm)	0.42
Percentage of water to cement (kg)	10-5
Special Weight (kg/m ³)	1800

3.2. How to make concrete

The amount of weight of the materials for the design of mixing light concrete for a certain amount of concrete in such a way as to provide the volume of concrete required to perform the tests was calculated and then the materials were weighed. These materials were poured into the concreting machine in the order of coarse grain (Lika), natural sand, cement and micro-silica, and the machine was kept on for 3-5 minutes to mix the dry materials without water. Then first, all the water and a part of the super-lubricant are gradually added to the dry materials inside the Betonir Roshan machine. Finally, the remaining amount of super-lubricant is added to ensure proper performance and the desired slump.

With numerous and preliminary experiments, it has been concluded that correct mixing, both in terms of mixing and mixing time, has a significant effect on the strength of concrete, therefore, the mixing time was based on this and with the appropriate number of rotations of the concrete Try to mix all the ingredients well. After finishing the mixing and making of concrete, some of the concrete is used to supply the slump. The produced concrete was poured into clean and lubricated cubic molds of 10x10x10

cm in three layers and each layer was vibrated for 20 seconds with the help of a vibrating table. After being vibrated for 16-24 hours, the samples were kept inside the mold with a damp cloth cover, and then they were removed from the molds with great care and without damaging the mold, and were kept in the water basin with water until the test. The temperature is maintained at $20 \pm 2^\circ\text{C}$.

3.3. Test to determine the compressive strength of hardened concrete

In general, two types of samples are used for compression testing, which are cubic and cylindrical. In England (English code, 2009) [8] and many European countries, cubic samples are used, in American standards (American concrete code and the standard for testing the compressive strength of cylindrical concrete samples) [9] and others Countries such as France and Australia are recommended examples of cylindrical shape. In this research, 10x10x10 cm cubic samples were used to determine the compressive strength.

To perform this test, the samples are poured into a steel or cast iron mold. The cubic shape of the molds, the size of the sides and the smoothness of the surfaces inside the mold must comply with the recommended specifications. In cases where the compaction is done by a vibrating device, it is necessary that the connection of the mold body to its bottom is rigid. The inner parts of the mold should be slightly greased with mold oil to prevent concrete from sticking to them. After pouring the concrete into the molds, it should be compacted. Compaction of cubic samples is done with a vibrating table or by hand. The cubes are filled in three layers and after each layer is poured, it is compacted. In compacting with a vibrating table, instead of pounding, after pouring each layer of concrete, the mold is placed on the vibrating table for a certain period of time until the concrete is completely compacted. After processing, the samples are taken out of the mold and kept in the water tank at a temperature of $20 \pm 2^\circ\text{C}$ before testing.

The samples are removed from the pond before the test and their surface is dried. Then, the tested cubic samples are placed between the two plates of the machine in such a way that the surface of the sample is in contact with the cubic mold. Now, a vertical

force is applied to the cubic sample by the device at a constant speed so that the cube is packed due to the compressive force. The force and tension corresponding to it are read and recorded from the digital screen of the device.

3.4. Construction of lightweight concrete beam samples made of Lika

All columns are made with a height of 100 cm and cross-sectional dimensions of 20 cm x 20 cm. All the columns have 4 rebars with a diameter of 10 mm and khamut with a diameter of 8 mm, which are placed at a distance of 75 mm to 150 mm from each other. The schematic of the compression test system and the details of the columns are presented in Figure 1.

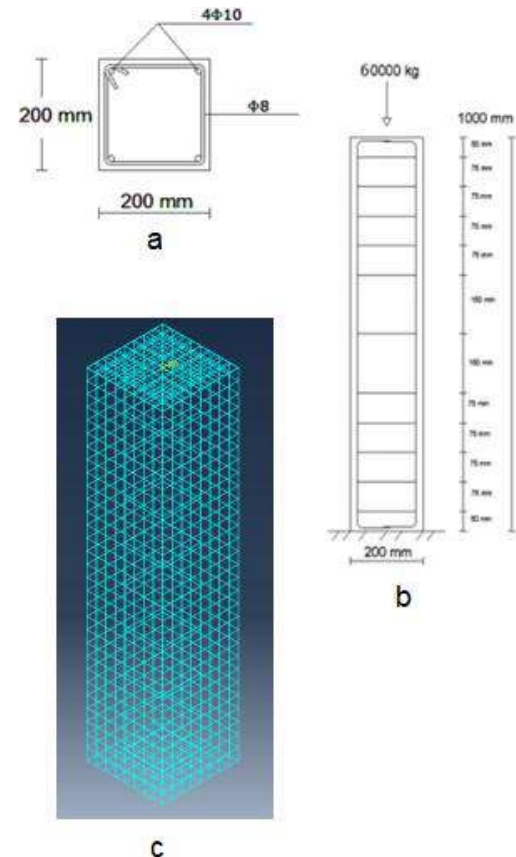


Fig 1. a and b) Schematic of the test system and details of the columns c) Column elementing modeled in Abqus software

3.5. How to perform the test and test the columns

According to Iran's concrete code, standard hooks are created on rebars and anchors, and in order for the anchors to be fixed, we tie them to the rebars with strong reinforcement wire, so that they do not move during vibration and are stable. After that, the molds were adjusted and fixed in the desired sizes, and the walls were coated with a thin layer of oil to prevent the concrete from sticking to the walls of the mold. Then the closed rebars were placed inside the mold and then concrete pouring was done according to the relevant mixing plan. In order to better compact the concrete, a special vibrator was used to vibrate the poured concrete. 24 hours after concrete pouring, while the columns were still in the mold, the surface that was in contact with the air was kept moist, and the columns were removed from the mold after 48 hours, and after being taken out of the mold, they were placed in a pool of water in the laboratory. All the columns were tested after 90 days from the date of concreting. To determine the direction of the cracks that are caused by the load, the surface of the column was covered with lime and after determining the exact location of the load, the location of the strain gauge was marked. After placing the column in the device, the load was introduced into the tested column by a jack with a capacity of 100 tons. In order to read the load (in Kg) and its related displacement, a load gauge and strain gauge were used, respectively, and for each amount of load applied by a manual jack, the corresponding load and displacement were read and recorded.

4. Checking the test results

Based on the application and physical properties, lightweight concrete is divided into three categories: lightweight concrete, semi-structural, and heat insulation, each of which has its own requirements (the lightweight requirements for use in lightweight structural concrete are given in ASTM C 330) and in the rest of this section, we will deal with the physical and structural characteristics of this type of concrete, which is the result of laboratory and theoretical results, and also examine and compare the results of finite element analysis using the modeling of samples

in ABAQUS software and compare with the laboratory results.

Concrete structures are among the strongest and safest structures. However, the unit weight of the high volume of concrete used causes an increase in the dead load of the structure, and its consequence is an increase in lateral loads caused by earthquakes. Therefore, the use of lightweight concrete can play a significant role in reducing the forces on the structure.

In the last decade, with the help of additives and super-lubricants, it is possible to produce lightweight concrete with high strength, the use of lightweight concrete in the construction of slabs, beams, and columns has expanded greatly. In bridges, where the weight of the beam creates lateral loads. It is relatively noticeable, the use of light concrete will have a great effect in reducing lateral loads. Also, in cases where for the purpose of repairing or strengthening the beam, the dimensions of the beam and as a result the weight of the structure increases a lot, the use of light concrete will be appropriate.

In this section, the structural behavior of the experimental and modeled column samples is investigated, the results of the compressive strength tests of the cubic samples and the compressive test of the columns are explained. Also, the load-displacement diagram of the columns is drawn. Next, the results of the analysis of finite elements using the modeling of the samples are mentioned in the software, and finally, a comparison is made between the laboratory and modeling results.

In order to investigate the structural behavior of the columns, five concrete columns were made, including light weight concrete with the same amount and arrangement of rebars, cross-sectional dimensions, the amount of cement and the ratio of water to cement, which are discussed in detail in section 3.

4.1. Investigating the structural behavior of laboratory columns

In Table 2, the results of the tests of Lika concrete columns are presented in order. In this section, the compressive behavior of columns is studied.

To investigate the change of location of the columns, the load-displacement curve is investigated. These curves are presented in Figure 2 and compared in the load-displacement results of the laboratory columns

with the result of the modeled sample. As it is clear in the figure, the curve of Lika light concrete columns is linear up to the load of 43645, 43256, 38550,

39745, 41880 kg respectively, but after that the slope of the curve decreases.

Table 2

Recorded values from the Leica light concrete column test

Column 1		Column 2		Column 3		Column 4		Column 5	
total load (kg)	column displacement (mm)	total load (kg)	column displacement (mm)	total load (kg)	column displacement (mm)	total load (kg)	column displacement (mm)	total load (kg)	column displacement (mm)
3960	0.26	3387	0.308	3548	0.28	3753	0.365	3790	0.48
7920	0.8	7430	0.65	7097	0.66	7506	0.698	8140	0.85
14500	1.85	13305	1.45	12774	1.35	13612	1.45	13486	1.65
18810	2.99	18275	2.52	16865	1.95	17775	1.81	20533	3.45
28512	5.27	25698	4.13	25427	3.8	26775	3.45	26200	5.52
34650	6.86	33695	6.3	31550	5.22	32850	4.85	32197	7.12
38550	8.85	36594	7.66	35650	6.85	36800	6.25	36520	8.23
43645	11.28	40270	10.3	38550	8.23	39745	8.55	41880	10.46
44550	14.53	43256	12.22	39860	11.35	41580	12.2	43132	13.22
46530	17.85	44050	15.06	40340	14.15	42856	15.1	44518	16.8
47720	21.33	44765	19.24	40950	17.9	43250	19.2	46170	19.8

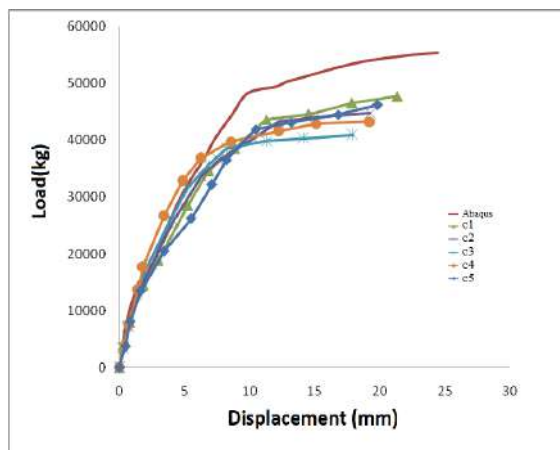


Fig 2. Load-displacement curve of columns and modeled in Abaqus software

The ultimate breaking load of Lika light concrete columns is 47720, 44765, 40950, 43250 and 46170 kg respectively. The comparison of the ultimate load of Leica light concrete shows that although its specific weight and compressive strength is lower

than ordinary concrete, it has an acceptable ultimate strength for use in a structural column. The weight of concrete, light concrete column of Leica with specific weight and average compressive strength of 24.18 MPa is about 25% less than the weight of ordinary concrete, which by making the weight of concrete lighter, significant benefits can be obtained, including reducing the forces on the structure. Finds

In Figure 3, the stress-strain curves of Lika light concrete columns are presented and compared with the modeled sample result. The stress created in the column is obtained by dividing the load applied to the sample by the cross section of the column. The strain created in the column is also obtained by dividing the displacement by the length of the sample.

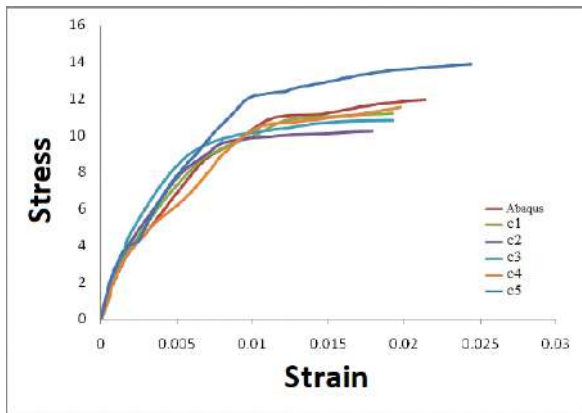


Fig 3: Stress-strain curve of columns modeled in Abaqus software

4.2. The results of the structural behavior of the modeled column and comparison with laboratory columns

In this research, the powerful Abaqus finite element software was used for modeling and static analysis on Lika light concrete column samples. Figure 2 shows the load-displacement diagram of the modeled column. Also, the displacement contour obtained for the column modeled in finite element software is shown in Figure 4.

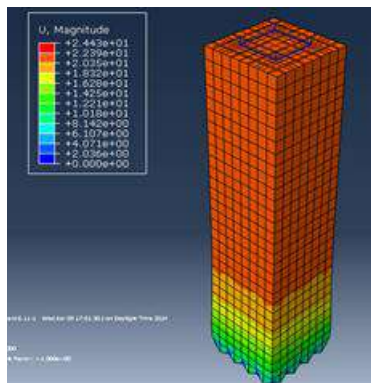


Fig 4. Displacement contour in the direction of force application

According to Figure 2, it can be seen that the modeling results agree with the experimental results with an acceptable approximation. According to the diagrams in Figure 2 and the final strength and displacement of the samples, it can be seen in the laboratory samples and the modeled samples that

there is an acceptable match between the results and the correctness of the software output results can be ensured.

The relations in the regulations are based on normal concrete, while the concrete used in this research is of light concrete type, so the bearing capacity obtained based on the relations is not necessarily similar to the laboratory results. In the laboratory, there is a possibility of execution errors, so the accuracy of the obtained results is lower than the result of modeling in Abaqus software.

Also, the main stress contour obtained for the column modeled in the finite element software is shown in Figure 5.

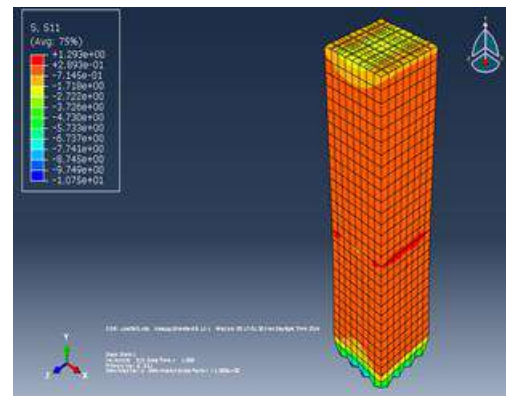


Fig 5. Main stress contour of the modeled column

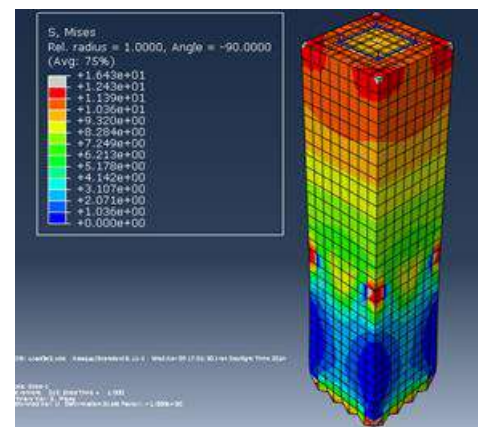


Fig 6. Mizez stress contour

According to Figure 3, it can be seen that the modeling results agree with the experimental results

with an acceptable approximation. As we know, cracks occur in places where the stress has reached the cracking stress of concrete. Therefore, the Von-Mises stress distribution of the columns is also shown

in Figure 6. On the other hand, the shape of the cracked column in the laboratory is also shown in Figure 7.

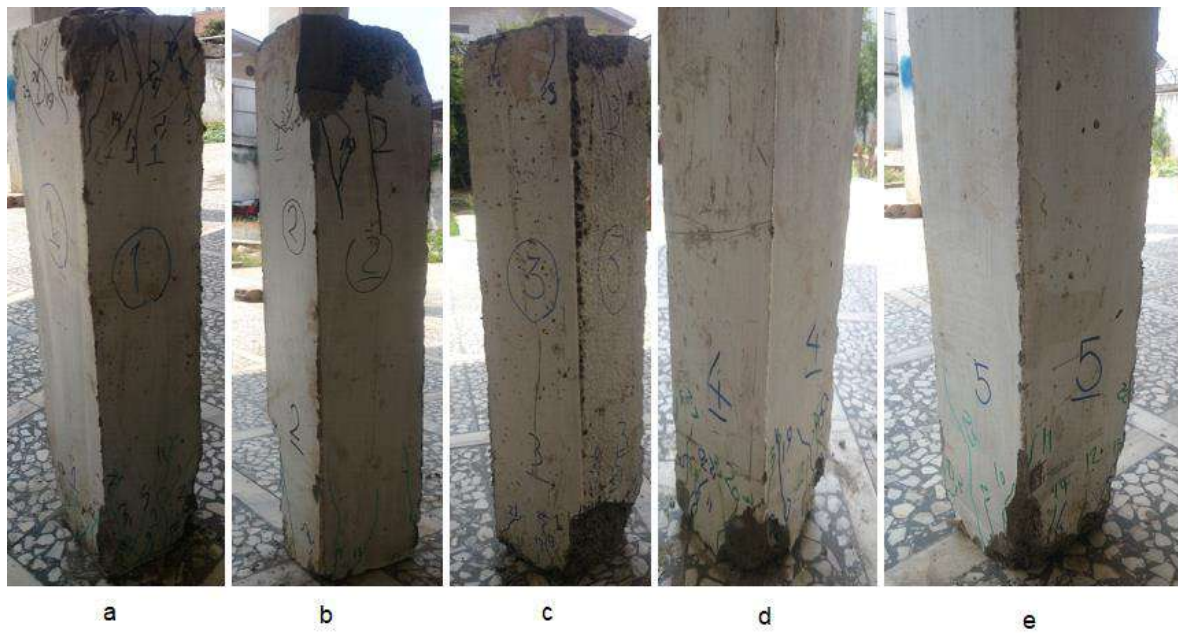


Fig 7. Showing the shape of the cracks after loading the right stones a) column 1 b) column 2 c) column 3 d) column 4 e) column 5

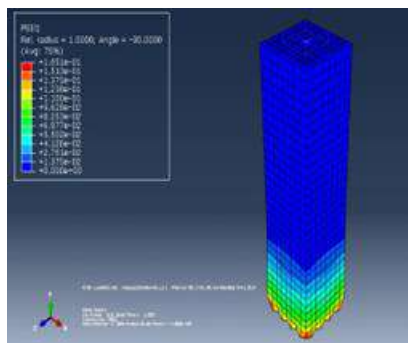


Fig 9. Plastic strain contour

By comparing the experimental results with the modeling results, we come to the conclusion that the shape of the crack corresponds to the stress distribution obtained from finite element analysis, and this is another proof of the accuracy of the modeling and the reliability of the model. On the

other hand, we know that at the moment of the final failure of the column, at the points where the plastic strain exceeds 0.0035, crushing occurs in the concrete. For this purpose, the plastic strain distribution of the concrete column is shown in Figure 9.

As can be seen in the figure, at the points where the strain exceeds the plastic strain of the concrete in the modeled column, crushing has occurred, that is, at the support location, which is consistent with the laboratory results shown in Figure 8. Matches

5. The result

This research deals with presenting the results of analytical and experimental studies on columns made of light-grained concrete under the effect of axial load. A total of 5 structural columns made of light-grained concrete were investigated in a laboratory

manner, and at the end, one column was modeled using Abaqus finite element software.

The load-displacement diagram of all the columns has been drawn, and the matching of these diagrams indicates that the columns have the same behavior under the effect of axial load. Stress-strain diagrams of all columns are drawn, which are similar to load-displacement diagrams. The final load that the built columns can bear is about 44.57 tons, and in this case, the displacement of the column is 19.5 mm. The model made in Abaqus finite element software has an acceptable agreement with the experimental results. The shape of the cracks in the laboratory samples corresponded with the stress distribution obtained from finite element analysis, and this is a proof of the accuracy of the modeling.

From the comparison of the results obtained in this research with the numerical results obtained by using the relations of the regulations that are for ordinary concrete, we come to the conclusion that the bearing capacity of the column with light concrete is less than that of ordinary concrete, but according to To reduce the weight of the sample and that this difference in capacity is negligible, it is recommended to use light concrete in structural members such as beams or columns.

References

- [1] Bagheri AS, Rahmani AS, Ruh Shahbaz J. 2001, Laboratory study of engineering properties of lightweight concrete made with natural lightweight aggregate (Pumice), the first international conference on concrete and development.
- [2] Yazdi J. "Lightweight concrete and its application in the construction industry", Tabriz Lightweight Insulation Industrial and Mining Company.
- [3] M. H. Myat, T. H. wee, behaviour of Spiral Reinforced Light weight Aggregate Concrete Columns, 32 nd Conference on our world in concrete & Structures, 2007.
- [4] Dante Galeota, Matteo M. Giammateo and Amedeo Gregori, Ductility and Strength in High- Performance Light weight Concret columns, 13th world conference on earth quake engineering 2004, August, Paper, No. 3414.
- [5] Y.C. Kan, L.H. Chen, C.H. Wu, C.H. Huang, T. Yen, and W.C. Chen, behaviour and Size effect of Light weight Aggregate Concrete Column under Axial load, 2010.
- [6] Shahdeh Ghannam, Orabi Al- Rawi and Moh'd El- Khatieb, experimental study on light weight concrete- Filled Steel Tubes, Jordan Jornal of Civil engineering, 2011, Volume 5, N. 4.
- [7] M. Mouli and H. Khelafi Strength of Short Composite Rectangular Hollow Section Columns Filled With light weight Aggregate Concrete, engineering Structures 29, 2007.
- [8] BSEN. 12390-3: 2009- Testing hardened Concrete Compressive Strength of test Specimens.
- [9] ASTM C39/C 39M- 14a. Standard test method for Compressive Strength of Cylindrical Concrete Specimens.



Parametric study of two-layer corrugated steel shear wall under lateral load

Saeid Ostai^{a*}

^aEngineering faculty, Chalous Branch, Islamic Azad University, Chalous, 46615-397, Iran

Abstract: Steel shear walls have always been used in the construction and improvement of many structures due to their advantages such as high strength and stiffness, ductility and excellent energy absorption. In the meantime, corrugated steel shear walls have been proposed due to postponing the elastic buckling of the plate and increasing ductility and energy absorption. Corrugated steel shear walls can be used in both single and double layers. Due to the fact that so far, limited research has been conducted about double corrugated steel shear walls, therefore, in this research, the hysteresis behavior of double and single layer corrugated steel shear walls has been analyzed parametrically using the finite element method and using ABAQUS software. Thus, after validating a experimental sample, a two-layer corrugated steel shear wall with one bay-one story with conventional angles of 30, 45 and 60 degrees was investigated in ABAQUS software under cyclic loading. The results of this research showed that the hysteresis curve of double and single layer corrugated steel shear walls is stable. Also, the resistance and energy absorption of double corrugated steel shear walls is higher than single layer corrugated wall. Also, the resistance of corrugated steel shear walls with single and double layers is lower than that of flat steel shear walls. Also, increasing the corrugation angle of the plate has led to an increase in resistance and energy absorption. In addition, behavior factor and ductility of flat steel shear walls are higher than single-layer and double corrugated walls. Nevertheless, the over-strength factor of the studied samples is almost equal to each other. © 2017 Journals-Researchers. All rights reserved. (DOI: <https://doi.org/10.52547/JCER.4.4.51>)

Keywords: Corrugated wall, resistance, energy absorption, seismic coefficients, abacus

1. Introduction

Steel shear wall to deal with the lateral forces of earthquake and wind in buildings, especially in tall buildings, has been considered in the last five decades. The steel shear wall system is a very simple system in terms of implementation and there is no special complexity in it. High resistance, high stiffness, high ductility and stable hysteresis behavior

are the main advantages of this system. Steel shear walls without stiffeners have lower strength and energy absorption due to premature buckling of the plate. To overcome this problem, two ways of using hardener and corrugated plate are suggested. So that the use of corrugated plate delays buckling and subsequently increases energy absorption and ductility, another solution that is the use of double corrugated plates. In this thesis, the behavior of double trapezoidal corrugated steel shear walls under cyclic loading will be investigated in ABAQUS

* Corresponding author. Tel.: +989119903830; e-mail: saeidosati99@gmail.com.

software. A lot of research has been done on corrugated steel shear walls in the past, some of which are briefly reviewed below. In 2021, Rudsari et al investigated the effect of opening characteristics and plate thickness on the performance of sinusoidal and trapezoidal corrugated steel shear walls [1]. In 2021, Wang et al analyzed the relationship between out-of-plane and in-plane failure of corrugated steel plate shear wall [2]. This paper examines the relationship between out-of-plane stiffness and in-plane stiffness in a frame shear wall with a boundary member including beam and column to achieve full in-plane performance. In 2021, Gohtarian and Melki conducted a numerical study of corrugated steel shear walls with double-layer plate [3]. In this research, things like horizontal or vertical orientation of the corrugated plate, connection of the plate to the columns, thickness of the plate and ratio of plate dimensions were investigated as the main parameters. The results of this research showed that corrugated steel shear walls with double-layer plates have considerable stiffness, resistance and energy dissipation capacity. In 2021, Joharchi et al. investigated the parametric periodic behavior of steel shear walls with corrugated plate [4]. Things such as plate corrugation angle, plate thickness and also the ratio of panel dimensions were investigated in this research. The results of this research showed that increasing the thickness of the plate led to an increase in stiffness, energy absorption and resistance. In addition, the effect of the corrugation angle of the plate depends on the thickness of the corrugated plate. In 2020, Behrebar et al investigated the behavior of corrugated steel shear walls with sinusoidal plate under the effect of cyclic loads [5]. In this article, the behavioral performance of sinusoidal corrugated steel shear walls with central opening has been investigated. In this research, it was shown that creating an opening and increasing its dimensions leads to a decrease in the performance of the system, which is due to a decrease in the share of the plate in the lateral load. In 2020, Bhorebar et al evaluated and predicted the response of steel shear walls with corrugated plate and beam with reduced section [6]. In this research, it was found that models with a corrugation angle of 45 degrees showed better performance in terms of energy absorption capacity. In 2019, Nouri and Iftikhar investigated numerically

the effect of the shape and location of the opening on the behavior of corrugated steel shear walls [7]. Kalantari and KalatJari in 2019 investigated the seismic performance of the proposed new system of steel shear wall composed of smooth and corrugated plates [8]. In 2018, Fazel et al investigated the effect of plate corrugation angle and its direction on the performance of corrugated steel shear walls [9]. In 2018, Wang et al investigated the seismic performance of composite steel shear walls with corrugated plate [10]. Caio and Huang in 2018 investigated the laboratory and numerical simulation of steel shear walls subjected to cyclic loads [11]. In 2018, Deva et al investigated the shear strength and post-buckling behavior of corrugated steel shear walls [12]. This paper has carried out numerical investigations on the behavior of lateral resistance and the design of corrugated infill plates in steel shear walls under uniform lateral shear force. In 2018, Qi et al investigated the laboratory behavior of corrugated steel shear walls [13]. Three corrugated walls and one wall with a flat plate were tested in this research. The bearing capacity of the wall with flat plate is higher than the wall with corrugated plate. This is despite the fact that the initial stiffness of the flat wall was lower than that of the wavy walls. In 2018, Tong and Gu investigated the behavior of corrugated steel shear walls containing hardener [14]. The results of this research showed that the presence of hardeners has been able to significantly prevent buckling out of the wall plane. It has also been able to increase the carrying capacity and plasticity. In 2017, Ding et al investigated the effects of opening on the behavior of trapezoidal corrugated steel shear walls [15]. In this article, in general, all the samples studied in this research showed good deformation capacity and plasticity. The results of this research also showed that the initial stiffness of the wall without openings is higher than the samples with openings. Also, the energy absorption of the sample without opening is less than the sample with opening. The cyclic behavior of corrugated steel shear walls with sinusoidal plate was investigated in 2017 by Zhao et al. [16]. The results of this research showed that the energy absorption, strength and initial stiffness of corrugated steel shear walls with a large depth are 26, 5 and 34% higher, respectively, compared to a simple plate shear wall. Meanwhile, the bearing capacity of a

flat wall is 25% higher than that of corrugated walls with a shallow depth. The direction of placing the corrugated plate inside the panel also has a small effect on the behavior of the sinusoidal corrugated walls. In 2017, Noor Alizadeh et al investigated the behavior of smooth steel shear walls reinforced by corrugated plates [17]. The results of this research showed that the maximum shear capacity of steel shear wall reinforced with corrugated plate is on average 31% higher than smooth steel shear walls. Also, the use of corrugated plate in the whole panel has no effect on preventing the buckling of the flat plate, and therefore it is not recommended to use the corrugated plate as a reinforcement in the whole panel. In 2017, Shun et al. experimentally investigated the cyclic behavior of corrugated steel shear frames [18]. The results of this research showed that the way of placing the corrugated plate horizontally or vertically inside the panel does not have much effect on the cyclic behavior of the corrugated walls. Hosseinzadeh et al investigated the behavior of corrugated steel shear walls in a laboratory in 2017 [19]. The main variable in this research was the plate corrugation angle. In this research, it was observed that by reducing the corrugation angle of the plate, the initial stiffness, load capacity and energy absorption increased. However, no significant relationship was found between the ductility coefficient and the corrugation angle of the plate. In 2016, Yoo and Yoo investigated the behavior of cold-rolled steel shear walls containing circular openings [20]. In this research, it was found that cold-rolled corrugated shear walls without opening have significantly high initial strength and stiffness, but they have poor ductility under cyclic loading. In 2013, Emami et al investigated the seismic performance of simple and corrugated steel shear walls [21]. The results of this research showed that the initial stiffness of walls with corrugated plates is higher than that of plain walls. Also, the bearing capacity of samples with corrugated plate is less than that of a simple wall. Corrugated plate samples showed up to 6% relative displacement and plain wall sample up to 5% relative displacement.

2. Research method

In this research, ABAQUS software will be used to model the studied samples. First, a one-story-one-bay steel shear wall frame with a flat plate was designed using Guide No. 20 of the AISC341 regulation, which is specific to steel shear walls, and then under cyclic loading, its hysteresis behavior was studied and the parameters of strength, stiffness and energy absorption were investigated. And also the seismic coefficients will be extracted. In the next step, behavior of single and double corrugated steel shear walls with the corrugation angle of 30, 45 and 60 degrees was studied. It should be noted that in order to investigate the effects of the thickness of the corrugated plate, three thicknesses of 2, 4 and 6 mm considered. ATC24 loading protocol has been used to study the cyclic behavior of the samples. The images of single-layer and double-layer corrugated wall sections are shown in figures 1 and 2, respectively:



Figure (1) cross-section of a single-layer corrugated wall



Figure (2) cross-section of a double-layer corrugated wall

3. Validation

In this section, the validation results are presented. The intended validation is related to the laboratory work of Emami et al., which is a corrugated steel shear wall sample [21]. They used the plate in figure 3 as a trapezoidal corrugated plate.



Figure (3) dimensions and wave geometry in corrugated steel shear wall [21]

Dynamic implicit method was used for cyclic analysis in ABAQUS software. In the application section. The hysteresis curve obtained from the finite element analysis along with the laboratory results is also shown in Figure 4. As can be seen in the figure, there is a very good agreement between the experimental results and the finite element analysis.

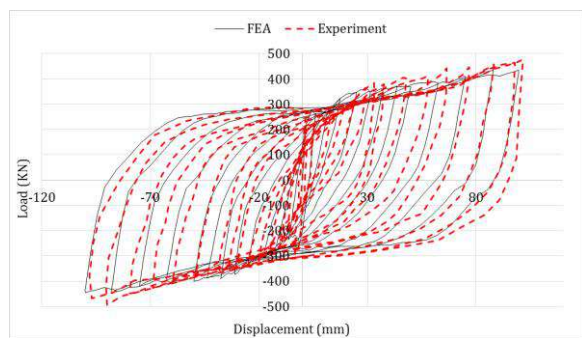


Figure (4) load-displacement curve of FE and test models

4. Modeling considerations in ABAQUS software

S4R type shell element has been used to model flat, corrugated plate and other members. Structured meshing technique has been used for various members of corrugated steel shear wall. In order to analyze the behavior of the studied samples in ABAQUS software, implicit dynamic analysis method has been used. In order to connect the infill plates to the boundary members including beams and columns, the tie option in the interaction module was used in ABAQUS software. it should be mentioned that the behavior of the steel used in the materials module in the strain hardening of Combined

5. Specifications of the studied samples

The geometric specifications of the studied frame are presented in Table 1. It should be mentioned that the I-shaped section is used for the beam and column members. d, bf, tf and tw in the mentioned tables mean height, flange width, flange thickness and web

thickness, respectively. The height of all floors is 3200 mm and the width of the frame is 5600 mm. It should be mentioned that ordinary steel St37 has been used for beam, column and plate members. The yield and ultimate stress of this steel were considered to be 240 and 360 MPa, respectively.

6. behavior of the studied samples

6.1. behavior of samples with a plate thickness of 2 mm

Figures 5 to 7 show the hysteresis curves of samples with a plate thickness of 2 mm

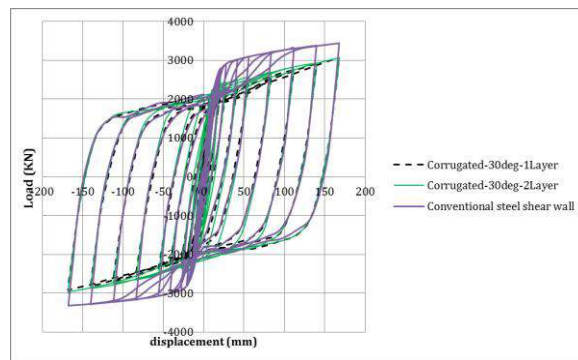


Figure (5) hysteresis curve of samples with a corrugation angle of 30 degrees and a plate thickness of 2 mm

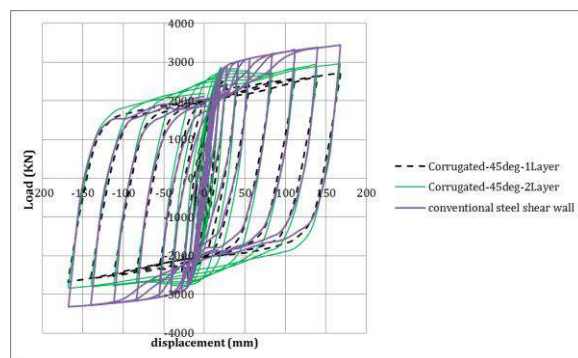


Figure (6) hysteresis curve of samples with a corrugation angle of 45 degrees and a plate thickness of 2 mm

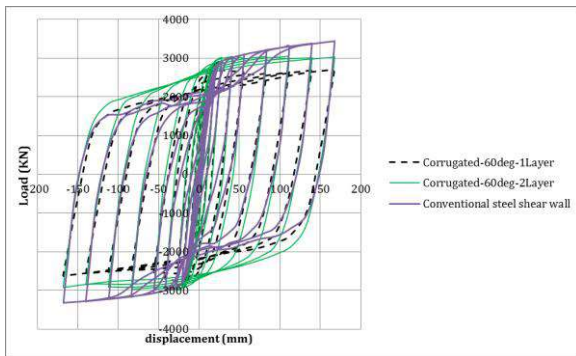


Figure (7) hysteresis curve of samples with a corrugation angle of 60 degrees and a plate thickness of 2 mm

Table 1 shows the maximum resistance values of corrugated and plain wall samples with 2 mm plate thickness. As can be seen, the resistance of corrugated walls with a 30-degree angle with single and double plate with a thickness of 2 mm is lower by 11.8% and 10.9%, respectively, than the flat steel shear wall. The resistance of corrugated walls with a 45 degree angle with single and double plates is lower than flat steel shear wall by 21.3 and 13.9 percent, respectively. Also, the resistance of single and double corrugated walls with an angle of 60 degrees is lower than flat steel shear wall by 14.6% and 11.6%, respectively. Another result is that, the resistance of the double corrugated wall with angles of 30, 45 and 60 degrees is 1, 9.4 and 3.6% higher than the single layer corrugated wall, respectively.

Table 1

Resistance of corrugated and plain wall samples with 2 mm plate thickness

sample	corrugation angle (degree)		
	30	45	60
2-layer corrugated steel shearwall	3066	2963	3042
1-layer corrugated steel shear wall	3035	2707	2937
Flat steel shear wall	3442		

In Table 2, the energy absorption values of

corrugated and flat wall samples with 2 mm plate thickness are presented. The absorbed energy of the single and double layer corrugated steel shear wall with a corrugation angle of 30 degree is lower by 10.8 and 1.3 percent, respectively, compared to the flat steel shear wall. The absorbed energy of the double corrugated wall with a corrugation angle of 45 degrees is 11.8% more than the flat steel shear wall. Meanwhile, the energy absorbed by the single-layer corrugated wall is 4.6% less than the simple steel shear wall. The absorbed energy of single and double corrugated walls with an angle of 60 degrees is more than the simple steel shear wall by 1.5 and 20.5%, respectively. Single layer is 10.6%, 19.5% and 18.7% respectively.

Table 2

Absorbed energy in corrugated and flat walls samples with 2 mm plate thickness

sample	corrugation angle (degree)		
	30	45	60
2-layer corrugated steel shearwall	4468	5065	5458
1-layer corrugated steel shear wall	4039	4237	4598
Flat steel shear wall	4529		

6.2. Behavior of samples with a plate thickness of 4 mm

Figures 8 to 10 show the hysteresis curves of samples with a plate thickness of 4 mm.

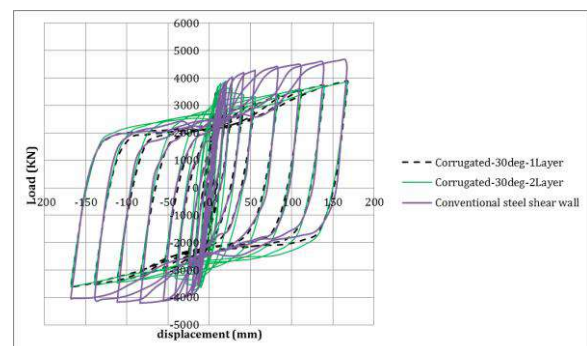


Figure (8) hysteresis curve of samples with a corrugation

angle of 30 degrees and a plate thickness of 4 mm

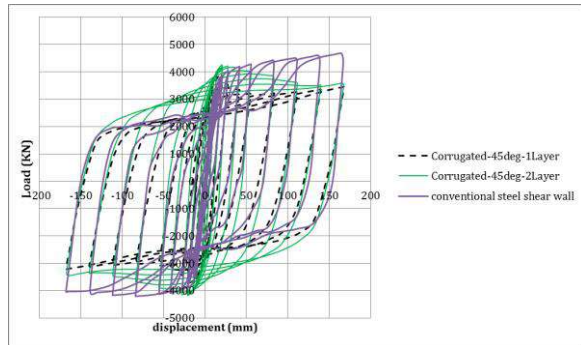


Figure (9) hysteresis curve of samples with a corrugation angle of 45 degrees and a plate thickness of 4 mm

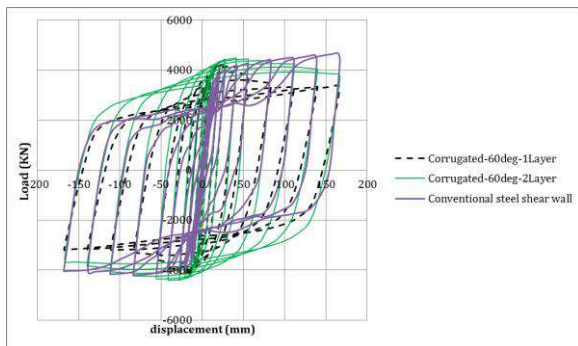


Figure (10) hysteresis curve of samples with a corrugation angle of 60 degrees and a plate thickness of 4 mm

Table 3 shows the maximum resistance values of corrugated and flat wall samples with 4 mm plate thickness. According to the values in Table 4, in the case of steel shear walls with a plate thickness of 4 mm, the results are as follows:

The maximum resistance of single and double layer corrugated steel shear wall with 30 degree corrugation angle is lower by 16.4% and 16.8% respectively compared to flat steel shear wall. The resistance of corrugated walls with a 45 degree angle with single and double plates is 16.7% and 8.9% less than flat steel shear wall, respectively. Also, the resistance of single and double corrugated walls with an angle of 60 degrees is lower by 1.8 and 1.4

percent, respectively, compared to flat steel shear wall. The resistance of the double corrugated wall with angles of 45 and 60 degrees is higher than the single layer corrugated wall by 9.4% and 4.3%, respectively. The resistance of the double corrugated wall with an angle of 30 degrees is 0.4% less than the single layer corrugated wall.

Table 3

Strength of corrugated and simple wall samples with 4 mm plate thickness

sample	corrugation angle		
	30	45	60
2-layer corrugated steel shear wall	3884	4254	4477
1-layer corrugated steel shear wall	3901	3889	4292
Flat steel shear wall	4670		

Table 4 shows the energy absorption values of corrugated and plain wall samples with 4 mm plate thickness. The absorbed energy of the double corrugated wall with a corrugation angle of 30 degrees is 10.9% more than the simple steel shear wall. Despite this, the absorbed energy of the single-layer corrugated wall is 1.8% lower than that of the simple steel shear wall. The absorbed energy of the double corrugated wall with a corrugation angle of 45 degrees is 24% more than that of the simple steel shear wall. The absorbed energy of the single-layer corrugated wall is 3.8% less than the simple steel shear wall. The absorbed energy of the double and single layer corrugated wall with a corrugation angle of 60 degrees is 10% and 41% higher than the simple steel shear wall, respectively. The absorbed energy in double corrugated walls with angles of 30, 45 and 60 degrees is 21, 28 and 27% higher than single layer corrugated wall, respectively.

Table 4

Absorbed energy in corrugated and flat wall samples with 4 mm plate thickness

sample	corrugation angle		
	30	45	60
2-layer corrugated steel shearwall	4468	5065	5458
1-layer corrugated steel shear wall	4039	4237	4598
Flat steel shear wall	4529		

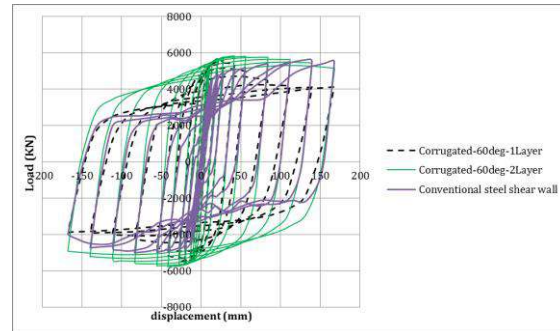


Figure (13) hysteresis curve of samples with a corrugation angle of 60 degrees and a plate thickness of 6 mm

6.3. Behavior of samples with a plate thickness of 6 mm

Figures 11 to 13 show the hysteresis curves of samples with a plate thickness of 6 mm.

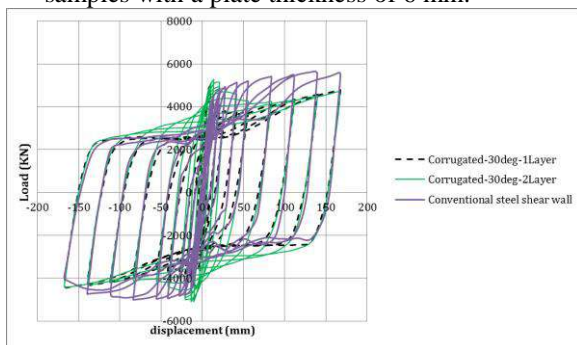


Figure (11) hysteresis curve of samples with a corrugation angle of 30 degrees and a plate thickness of 6 mm

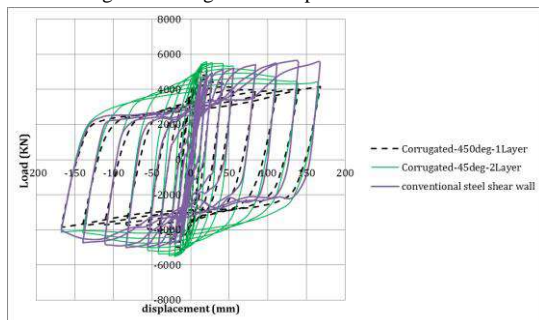


Figure (12) hysteresis curve of samples with a corrugation angle of 45 degrees and a plate thickness of 6 mm

In table 5, the maximum resistance values of corrugated and flat wall samples with 6 mm plate thickness are presented. According to the values in Table 6, in the case of steel shear walls with a plate thickness of 6 mm, the results are as follows:

- The maximum strength of single and double layer corrugated steel shear wall with 30 degree corrugation angle is lower by 12.6% and 6.75% respectively compared to plain steel shear wall.

- The resistance of corrugated walls with a 45-degree angle with single and double plates is 4.5% and 1.3% less than plain steel shear wall, respectively.

- The resistance of a single-layer corrugated wall with a 60-degree angle is 0.15% less than a simple steel shear wall. Meanwhile, the double corrugated wall is 2.3% more than the simple steel shear wall.

The resistance of the double corrugated wall with angles of 30, 45 and 60 degrees is higher than the single layer corrugated wall by 6.7%, 4.3% and 3.4% respectively.

Table 5

Strength of corrugated and simple wall samples with 6 mm plate thickness

Sample	Corrugation angle (degree)		
	30	45	60
2-layer corrugated steel shearwall	5274.92	5580.87	5839.94
1-layer corrugated steel shear wall	4944.33	5347.56	5648.34
Flat steel shear wall	5657.18		

In Table 6, the energy absorption values of corrugated and plain wall samples with 6 mm plate thickness are presented.

- The absorbed energy of the double corrugated wall with a corrugation angle of 30 degrees is 13% more than the simple steel shear wall. Despite this, the absorbed energy of the single-layer corrugated wall is 3.8% lower than that of the plain steel shear wall.

- The absorbed energy of the double and single layer corrugated wall with a corrugation angle of 45 degrees is 1 and 35% higher than the simple steel shear wall, respectively.

- The absorbed energy of the double and single layer corrugated wall with a corrugation angle of 60 degrees is 18% and 57% higher than the simple steel shear wall, respectively.

- The absorbed energy in double corrugated walls with angles of 30, 45 and 60 degrees is 23, 34 and 32% higher than the single layer corrugated wall, respectively.

Table 6

Strength of corrugated and simple wall samples with 6 mm plate thickness

Sample	Corrugation angle (degree)		
	30	45	60
2-layer corrugated steel shearwall	7944	9553	11038
1-layer corrugated steel shear wall	6445	7092	8326
Flat steel shear wall	7030		

7. Seismic coefficients of the studied samples

Tables 8 to 10 show the values of seismic coefficients in corrugated and plain wall samples with plate thickness of 2, 4 and 6 mm. As stated in the mentioned tables, the values of behavior coefficients and plasticity of smooth steel shear walls

are higher than single and double layer corrugated walls. Nevertheless, the added resistance factor of the studied samples is almost equal to each other.

8. Conclusion

The results of the numerical modeling done in this thesis are as follows:

- o ABAQUS software has a remarkable ability to predict the behavior of corrugated steel shear wall.

- o The values of coefficients of behavior and plasticity of smooth steel shear walls are higher than single and double layered corrugated walls. Nevertheless, the added resistance factor of the studied samples is almost equal to each other.

- o The resistance of corrugated steel shear walls, both single and double layer, is lower than plain steel shear wall. Only the resistance of the double-layer corrugated wall with a corrugation angle of 60 degrees and a thickness of 6 mm was higher than that of the plain wall.

- o The resistance of double-layer corrugated steel shear walls is higher than that of single-layer corrugated steel shear walls.

- o Energy absorption of double-layer corrugated steel shear wall is more than plain steel shear wall.

- o Energy absorption of double-layer corrugated steel shear wall is more than single-layer corrugated steel shear wall.

- o Increasing the angle of the corrugated plate has increased the strength and energy absorption of the single and double layer corrugated steel shear wall.

Acknowledgments

Acknowledgments should be inserted at the end of the paper, before the references, not as a footnote to the title. Use an unnumbered section heading for the Acknowledgments, similar to the References heading.

References

- [1] P. Audebert, P. Hapiot, J. Electroanal. Chem. 361 (1993) 177.
- [2] J. Newman, Electrochemical Systems, 2nd ed., Prentice-Hall, Englewood Cliffs, NJ, 1991.
- [3] A.R. Hillman, in: R.G. Linford (Ed.), Electrochemical Science and Technology of Polymers, vol. 1, Journals-Researchers, IRAN, 1987, Ch. 5.
- [4] B. Miller, Proc. 6th Australian Electrochem. Conf., Geelong, Vic., 19-24 Feb., 1984; J. Electroanal. Chem., 168 (1984) 91.
- [5] Jones, personal communication, 1992.
- [1] Sajjad Sayyar Roudsari, Sayed M. Soleimani, Sameer, Hamoushc Analytical study of the effects of opening characteristics and plate thickness on the performance of sinusoidal and trapezoidal corrugated steel plate shear walls, Journal of Constructional Steel Research 182 (2021) 106660
- [2] Wei Wang, Qirui Luo, Zhuangzhuang Sun, Bingjie Wang, Shanwen Xu, Relation analysis between out-of-plane and in-plane failure of corrugated steel plate shear wall
- [3] S.M. Ghodrati-Kashan, S. Maleki, Numerical Investigation of Double Corrugated Steel Plate Shear Walls, Journal of Civil Engineering and Construction 2021; 10(1):44-58
- [4] Ali Joharchi, Siti Aminah Osman, Mohd Yazmil Md Yatim, Mohammad Ansari, Numerical Parametric Study on the Cyclic Performance of Trapezoidally Corrugated Steel Shear Walls, Civil Engineering and Architecture 9(2): 462-476, 2021
- [5] Jing-Zhong Tong, Yan-Lin Guo, Wen-Hao Pan, Ultimate shear resistance and post-ultimate behavior of double-corrugated-plate shear walls, Journal of Constructional Steel Research 165 (2020) 105895
- [6] Milad Bahrebar, James B.P. Lim, George Charles Clifton, Tadeh Zirakian, Amir Shahmohammadi, Mohammad Hajsadeghi, Perforated steel plate shear walls with curved corrugated webs under cyclic loading, Structures 24 (2020) 600–609
- [7] نوری، غلامرضا، افتخار، غلامحسین. (1399). ارزیابی عددی تأثیر شکل و محل بازشو بر رفتار دیوارهای برشی فولادی موجدار. نشریه مهندسی سازه و ساخت، 7(4)، 78-92
- [8] کلانتري، اميد، کلات جاري، وحيد رضا. (1399). بررسی عملکرد لرزی سیستم نوین پیشنهادی دیوار برشی فولادی مرکب از ورق های صاف و موج دار. مهندسی عمران، 36.2(2.2)، 3-12
- [9] Hayder Fadhil, Amer Ibrahim, Mohammed Mahmood, Effect of Corrugation Angle and Direction on the Performance of Corrugated Steel Plate Shear Walls, Civil Engineering Journal Vol. 4, No. 11, November, 2018
- [10] Wei Wang | Yingzi Ren | Bin Han | Tan Ren | Gewei Liu | Yujian Liang, Seismic performance of corrugated steel plate concrete composite shear walls, Struct Design Tall Spec Build. 2018, Volume28, Issue1, e1564
- [11] Qiang Cao, Jingyu Huang, Experimental study and numerical simulation of corrugated steel plate shear walls subjected to cyclic loads, Thin-Walled Structures 127 (2018) 306–317
- [12] Chao Dou, Yong-Lin Pi, Wei Gao, Shear resistance and post-buckling behavior of corrugated panels in steel plate shear walls, Thin-Walled Structures 131 (2018) 816–826
- [13] Jing Qiu, S.M. Qiuhong Zhao, Cheng Yu and Zhongxian Li, Experimental Studies on Cyclic Behavior of Corrugated Steel Plate Shear Walls, J. Struct. Eng., 2018, 144(11)
- [14] Jing-Zhong Tong, Yan-Lin Guo, Shear resistance of stiffened steel corrugated shear walls, Thin-Walled Structures 127 (2018) 76–89
- [15] Yang Ding, En-Feng Deng, Liang Zong, Xiao-Meng Dai, Ni Lou, Yang Chen, Cyclic tests on corrugated steel plate shear walls with openings in modularized-constructions, Journal of Constructional Steel Research 138 (2017) 675–691
- [16] QiuHong Zhao, Junhao Sun, Yanan Li, Zhongxian Li, Cyclic analyses of corrugated steel plate shear walls, Struct Design Tall Spec Build. 2017; e1351
- [17] Amin Nooralizadeh, Morteza Naghipour, Mahdi Nematzadeh, and Hamed Zamenian, Experimental Evaluation of Steel Plate Shear Walls Stiffened with Folded Plates, International Journal of Steel Structures 17(1): 291-305 (2017)
- [18] Sudeok Shon, Mina Yoo and Seungjae Lee, (2017). An Experimental Study on the Shear Hysteresis and Energy Dissipation of the Steel Frame with a Trapezoidal-Corrugated Steel Plate, Materials, 10, 261
- [19] Hosseinzadeh, L., Emami F. and Mofid, M., (2017) "Experimental investigation on the behavior of corrugated steel shear wall subjected to the different angle of trapezoidal plate, The Structural Design of Tall and Special Buildings 26(17)
- [20] C. Yu, G. Yu, Experimental investigation of cold-formed steel framed shear wall using corrugated steel sheathing with circular holes, J. Struct. Eng. 142 (12.04016126), (2016)
- [21] Emami, F., Mofid, M., Vafai, A. (2013). Experimental study on cyclic behavior of trapezoidally corrugated steel shear walls, Journal of Engineering Structures, 48, 750–762

Author Guidelines EditEdit Author Guidelines

GENERAL GUIDELINES FOR AUTHORS

Journal of civil engineering researches invites unsolicited contributions of several forms: articles, reviews and discussion articles, translations, and fora. Contributions should fall within the broad scope of the journal, as outlined in the statement of scope and focus. Contributors should present their material in a form that is accessible to a general anthropological readership. We especially invite contributions that engage with debates from previously published articles in the journal.

Submissions are double-blind peer-reviewed in accordance with our policy. Submissions will be immediately acknowledged but due to the review process, acceptance may take up to three months. Submissions should be submitted via our website submission form (see links above for registration and login). Once you login, make sure your user profile has "author" selected, then click "new submission" and follow the instructions carefully to submit your article. If problems arise, first check the FAQ and Troubleshooting guide posted below. If you are still experiencing difficulty, articles can be submitted to the editors as email attachments.

Each article should be accompanied by a title page that includes: all authors' names, institutional affiliations, address, telephone numbers and e-mail address. Papers should be no longer than 10,000 words (inclusive of abstract 100-150 words, footnotes, bibliography and notes on contributors), unless permission for a longer submission has been granted in advance by the Editors. Each article must include a 100 words "note on contributor(s)" together with full institutional address details, including email address. We request that you submit this material (title page and notes on the contributors) as "supplementary files" rather than in the article itself, which will need to be blinded for peer-review.

We are unable to pay for permissions to publish pieces whose copyright is not held by the author. Authors should secure rights before submitting translations, illustrations or long quotes. The views expressed in all articles are those of the authors and not necessarily those of the journal or its editors. After acceptance, authors and Special Issue guest editors whose institutions have an Open Access library fund must commit to apply to assist in article production costs. Proof of application will be requested. Though publication is not usually contingent on the availability of funding, the Journal is generally under no obligation to publish a work if funding which can be destined to support open access is not made available.

Word template and guidelines

Our tailored Word template and guidelines will help you format and structure your article, with useful general advice and Word tips.

(La)TeX template and guidelines

We welcome submissions of (La)TeX files. If you have used any .bib files when creating your article, please include these with your submission so that we can generate the reference list and citations in the journal-specific style

Artwork guidelines

Illustrations, pictures and graphs, should be supplied with the highest quality and in an electronic format that helps us to publish your article in the best way possible. Please follow the guidelines below to enable us to prepare your artwork for the printed issue as well as the online version.

Format: TIFF, JPEG: Common format for pictures (containing no text or graphs).

EPS: Preferred format for graphs and line art (retains quality when enlarging/zooming in).

Placement: Figures/charts and tables created in MS Word should be included in the main text rather than at the end of the document.

Figures and other files created outside Word (i.e. Excel, PowerPoint, JPG, TIFF, EPS, and PDF) should be submitted separately. Please add a placeholder note in the running text (i.e. "[insert Figure 1.]")

Resolution: Rasterized based files (i.e. with .tiff or .jpeg extension) require a resolution of at least 300 dpi (dots per inch). Line art should be supplied with a minimum resolution of 800 dpi.

Colour: Please note that images supplied in colour will be published in colour online and black and white in print (unless otherwise arranged). Therefore, it is important that you supply images that are comprehensible in black and white as well (i.e. by using colour with a distinctive pattern or dotted lines). The captions should reflect this by not using words indicating colour.

Dimension: Check that the artworks supplied match or exceed the dimensions of the journal. Images cannot be scaled up after origination

Fonts: The lettering used in the artwork should not vary too much in size and type (usually sans serif font as a default).

Authors services:

For reformatting your manuscript to fit the requirement of the Journal of Civil Engineering Researchers and/or English language editing please send an email to the following address:

researchers.services@gmail.com

Noted: There is a fixed charge for these mentioned services that is a function of the manuscript length. The amount of this charge will be notified through a reply email.

FAQ AND TROUBLESHOOTING FOR AUTHORS

I cannot log in to the system. How do I acquire a new user name and password?

If you cannot remember your username, please write an email to (journals.researchers@gmail.com), who will locate your username and notify you. If you know your username, but cannot remember your password, please click the "Login" link on the left-hand menu at homepage. Below the fields for entering your username and password, you will notice a link that asks "Forgot your password?"; click that link and then enter your email address to reset your password. You will be sent an automated message with a temporary password and instructions for how to create a new password. TIP: If you do not receive the automated email in your inbox, please check your SPAM or Junk Mail folder. For any other issues, please contact our Managing Editor, Kamyar Bagherinejad (admin@journals-researchers.com).

How do I locate the online submission form and fill it out?

First you need to register or login (see above). Once you are logged in, make sure the "roles" section of your profile has "Author" selected. Once you assign yourself the role of "Author," save your profile and then click the "New Submission" link on your user home page.

Once you arrive at the submission form page, please read the instructions carefully filling out all necessary information. Unless specified otherwise by the editors, the journal section to be selected for your submission should be "Articles." Proceed to the remaining sections, checking all boxes of the submission preparation checklist, and checking the box in the copyright notice section (thus agreeing to journals-researchers's copyright terms). Once the first page is completed, click "Save and Continue." The next page allows you to upload your submission. Use the form to choose your file from your computer. Make sure you click "Upload." The page will refresh and you may then click "Save and Continue." You will then proceed to a page for entering the metadata for your article. Please fill out all required fields and any further information you can provide. Click "Save and Continue." The next page allows you to upload supplementary files (images, audiovisual materials, etc.). These are not required, but if you wish to provide supplementary materials, please upload them here (do not forget to click "Upload." Then click "Save and Continue." This brings you to the final page of the submission form. Please click "Finish Submission" in order to close the

submission process. You will then be notified by email that your article has been successfully submitted. TIP: If you do not receive the automated email in your inbox, please check your SPAM or Junk Mail folder. For any other issues, please contact our Managing Editor, Kamyar Bagherinejad (admin@journals-researchers.com).

Why am I not receiving any email notifications from HAU?

Unfortunately, some automated messages from Open Journal Systems arrive in users' Spam (or Junk Mail) folders. First, check those folders to see if the message was filtered into there. You may also change the settings of your email by editing your preferences to accept all mail from [jcer] and related journals-researchers.com email accounts.

I am trying to upload a revised article following an initial round of peer-review, but I cannot locate where to upload the article. Where do I submit a revised article?

Follow the login process outlined above and when you successfully login you will see on your user home page a link next to "Author" for "active" articles in our system (usually it is only one article, but if you have multiple submissions currently in our system, the number could be higher. Click the "Active" link and you will be led to a page that lists your authored articles currently in our system. Click the link under the column labeled "Status" and this will take you to a page showing the current review status of your article. At the very bottom of the screen, you will see an upload form under the heading "Editor decision." Here you may upload your revised article. An automated email will be sent to the editors and you may also notify them directly via email. You may then logout.

I successfully submitted an article; how long will it take for the editors to respond to me with a decision.

For all articles that are recommended for peer-review, the editors of JCER strive to notify authors of a decision within 4-6 weeks. You may contact JCER's Managing Editor, Kamyar Bagherinejad (admin@journals-researchers.com). if you have any questions relating to the review process and its duration.

For all other inquiries, please contact: Kamyar Bagherinejad (Managing Editor)

Privacy Statement

The names and email addresses entered in this journal site will be used exclusively for the stated purposes of this journal and will not be made available for any other purpose or to any other party.

Articles

Section default policy

Make a new submission to the Articles section.

Copyright Notice EditEdit Copyright Notice

Journal of Civil Engineering Researchers follows the regulations of the International Committee on Publication Ethics (COPE) and the ethical principles of publishing articles in this journal are set based on the rules of this committee, and in case of problems, it will be treated according to these rules.

This work is licensed under a Creative Commons Attribution 4.0 International License (CC BY 4.0).

In short, copyright for articles published in this journal is retained by the authors, with first publication rights granted to the journal. By virtue of their appearance in this open access journal, articles are free to use, with proper attribution and link to the licensing, in educational, commercial, and non-commercial settings

Privacy Statement EditEdit Privacy Statement

The names and email addresses entered in this journal site will be used exclusively for the stated purposes of this journal and will not be made available for any other purpose or to any other party.

Scholars Pavilion



Scholars Pavilion or **Scholars Chartagi** is a monument donated by the Islamic Republic of Iran to the United Nations Office at Vienna. The monument architecture is claimed by the Islamic Republic News Agency of Iran to be a combination of Islamic and Achaemenid architecture, although the latter clearly predominates in the decorative features, with Persian columns and other features from Persepolis and other remains from the Achaemenid dynasty. The Chahartaq pavilion form runs through the architecture of Persia from pre-Islamic times to the present.

Statues of four famous Persian medieval scholars, Omar Khayyam, Al-Biruni, Muhammad ibn Zakariya al-Razi and Ibn-Sina are inside the pavilion. This monument donated in June 2009 in occasion of Iran's peaceful developments in science.



J-Researchers